



Sedimentology and the facies architecture of the Ghaggar-Hakra Formation, Barmer Basin, India: Implications for early Cretaceous deposition on the north-western Indian Plate margin

Hazel Beaumont¹ | Stuart M. Clarke¹ | Stuart D. Burley^{1,2} | Andrew M. Taylor³ | Pinakadhar Mohapatra⁴

¹Basin Dynamics Research Group, School of Geography, Geology and the Environment, Keele University, Staffordshire, UK

²Orient Petroleum Limited, Islamabad, Pakistan

³Skolithos Ltd., The White House, Lancashire, UK

⁴Cairn India Ltd., DLF Atria, Gurgaon, India

Correspondence

Hazel Beaumont, Department of Geography and Environmental Management, University of the West of England Bristol, Bristol, UK.
Email: hazel.beaumont@uwe.ac.uk

Funding information

Keele University Acorn Fund; Cairn India Limited

Abstract

Fluvial strata of the Lower Cretaceous Ghaggar-Hakra Formation are exposed in fault blocks on the central-eastern margin of the Barmer Basin, Rajasthan. The sedimentology of these outcrops are described from 114 logs (thicknesses up to 100 m) and 53 two-dimensional correlation panels. The formation comprises three distinct channel belt sandstone packages defined as the Darjaniyon-ki Dhani, Sar-noo and Nosar sandstones separated by thick siltstone-dominated floodplain successions. The sediments were deposited in a sub-tropical, low sinuosity fluvial system that matures into a highly sinuous fluvial system. The Nosar Sandstone, the youngest of the three packages, exhibits a significant increase in energy and erosive power compared to those underlying it. This distinct change in fluvial style is interpreted as being rejuvenation due to an actively developing rift network forming accommodation space, rather than climatic controls acting on part of the depositional system. Consequently, the Ghaggar-Hakra Formation at outcrop represents Lower Cretaceous syn-rift deposition within the Barmer Basin with active localized fault movement from Nosar Sandstone times onward. These findings provide sedimentological evidence in support of pre-Palaeogene north-west–southeast extension in the Barmer Basin. Moreover, they imply Cretaceous extension took place widely along the northern extremity of the West Indian Rift System consistent with plate tectonic models of the break-up of Gondwana and evolution of the Indian Ocean. Outcrops of Lower Cretaceous strata are patchy across India and Pakistan. This study provides valuable material which, when combined with the available published data, facilitates a re-evaluation of Lower Cretaceous palaeogeography for the north-west Indian Plate. The reconstruction demonstrates a complex fluvial system, where the sediments are preserved sporadically as early syn-rift strata. The findings imply a high preservation potential for early Cretaceous fluvial successions within rifted fault blocks near Saraswati and Aishwarya of the Barmer Basin beneath the Palaeogene fill that likely have significant potential for further hydrocarbon exploration.

This is an open access article under the terms of the Creative Commons Attribution License, which permits use, distribution and reproduction in any medium, provided the original work is properly cited.

© 2018 The Authors. *The Depositional Record* published by John Wiley & Sons Ltd on behalf of International Association of Sedimentologists.

KEYWORDS

Barmer Basin, fluvial, Ghaggar-Hakra Formation, palaeogeography, tectonics

1 | INTRODUCTION

The Barmer Basin is the northern most basin of a series of rifts that comprise the West Indian Rift System (WIRS; Figure 1a), and hosts large hydrocarbon reserves within continental sediments of the basin fill (Dolson et al., 2015). However, the early geological history of the basin, and the nature of the Mesozoic sedimentary fill, remains poorly understood. This lack of knowledge stems mostly from the limited surface exposure which restricts outcrop studies and thereby constrains interpretations of subsurface well and seismic data.

The Barmer Basin was considered to have developed in response to passage of the Indian Plate over the Reunion hotspot, giving rise to a syn- and post-rift Palaeogene to Eocene sedimentary fill, overlying Precambrian rocks of the Malani Igneous Suite (Figure 2a, Crawford & Compton, 1969) and pre-rift Mesozoic sediments (Compton, 2009; Sisodia & Singh, 2000). Recently, an important earlier northwest–southeast extensional event has been

recognized, preserved in structural geometries exposed on the basin margins and overprinted by the perceived main Palaeogene rifting (Bladon, Clarke, & Burley, 2015; Dasgupta & Mukherjee, 2017). Fluvial sediments preserved on the rift margin are ascribed to the Lower Cretaceous Ghaggar-Hakra Formation and rift margin geometries suggest that they were deposited contemporaneously with the pre-Palaeogene normal faulting (Bladon, Burley, Clarke, & Beaumont, 2015; Bladon, Clarke, et al., 2015). Although the Ghaggar-Hakra Formation occurs in relatively small outcrops around Sarnoo, they are regionally significant as they provide excellent exposures of the early Cretaceous sediments which document intraplate continental deposition during the early break-up of India from Gondwana. It follows that the Ghaggar-Hakra Formation is likely to be the time and depositional-equivalent of the Lower Cretaceous fluvial Himatnagar Sandstone of the Cambay Basin (Bhatt, Solanki, Prakash, & Das, 2016; Mohan, 1995; Mukherjee, 1983), the fluvial to marine Nimar Sandstone of the Narmada Basin (Ahmad, 1988), the fluvial to coastal and

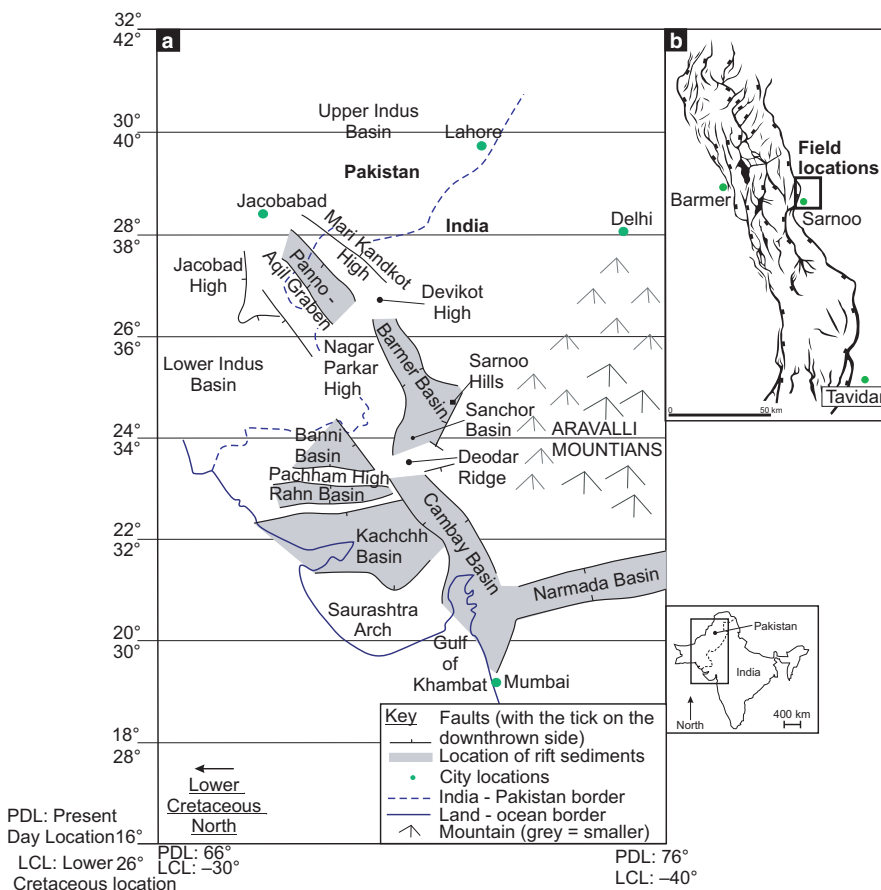


FIGURE 1 (a) Onshore rift basins within the WIRS (adapted from Balakrishnan, Unnikrishnan, & Murty, 2009) and various locations mentioned in the text: Inset gives the location of the Barmer Basin indicated by the solid black line within the Barmer District. (b) Principal extensional faults that define the geometry and limits of the Barmer Basin (adapted from Dolson et al., 2015), displaying the field locations for this study on the eastern, central margin. The settlement of Sarnoo is shown

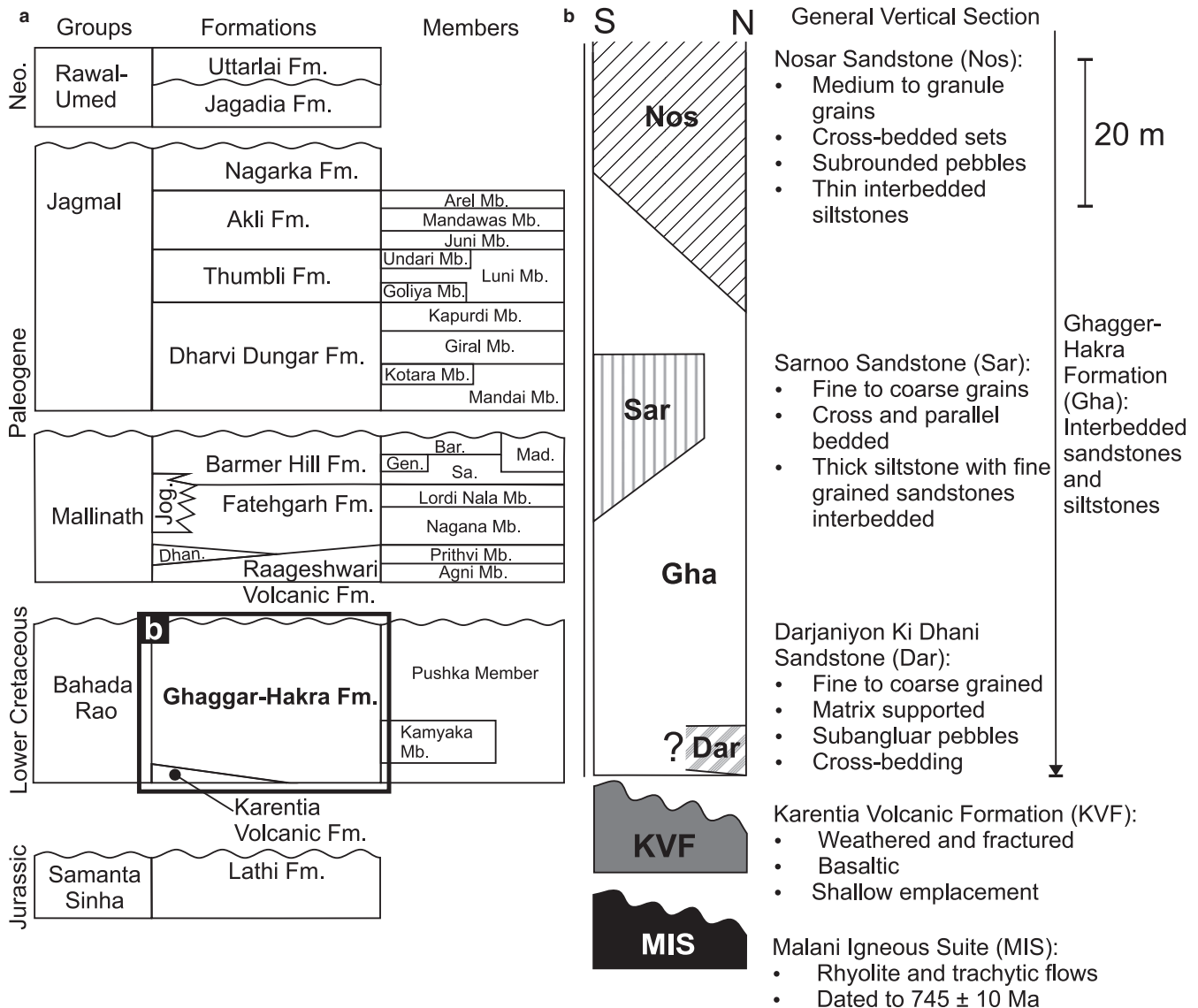


FIGURE 2 (a) Generalized vertical section of the Barmer Basin, displaying currently accepted group formations and members; Dhan. = Dhandlawas Formation, Jog. = Jogmaya Mandir Formation, Sa. = Sarovar Member, Gen. = Genhu hill Member, Mad. = Madpura Member, Bar. = Bariyada Member (Compton, 2009; Dolson et al., 2015; Sisodia & Singh, 2000; Tabaei & Singh, 2002; Tripathi et al., 2009); (b) generalized vertical section of the Ghaggar-Hakra Formation, displaying the separate lithostratigraphically informal sandstone units recognized by previous authors (adapted from Bladon, Burley, et al. 2015)

deltaic Bhuj Formation of the Kachchh Basin (Akhtar & Ahmad, 1991; Biswas, 1987; Desai & Desai, 1989), the predominantly fluvial Dhrangadhra Group of the Than Basin in Saurashtra (Casshyap & Aslam, 1992) and the fluvial Lumshiwal and Goru and marine-coastal Sembar successions of the Central and Southern Indus basins of Pakistan (Ahmad, Fink, Sturrock, Mahmood, & Ibrahim, 2012; Ahmad & Khan, 2012; Khalid, Qayyum, & Yasin, 2014; Zaigham & Mallick, 2000). These basin margin early Cretaceous sediments are likely to be contemporary with rifting between Madagascar and India (Bastia, Reeves, Pundarika, D'Silva, & Radhakrishna, 2010; Reeves, 2014; Torsvik et al., 2000) and separation of the Seychelles

microcontinent from Greater India (Eagles & Hoang, 2014).

Therefore, the Ghaggar-Hakra Formation and these isolated occurrences of fluvial sediments are important in reconstructing the Lower Cretaceous depositional palaeogeography of the north-western Indian Plate. Identification and detailed characterization of a well-preserved fluvial succession of Lower Cretaceous age in the Barmer Basin not only has significant implications for the evolution of the basin, but also for potential reservoir distribution and hydrocarbon potential of early Cretaceous sediments in the subsurface across the northern Indian Plate.

Here, a comprehensive description and interpretation of the Lower Cretaceous Ghaggar-Hakra Formation exposed in the Sarnoo and adjacent hills close to the settlements of Sarnoo (also known as Sarnu or Saranu), Karentia and Nosar, Rajasthan (Figure 1b) is presented as a basis for re-evaluating the early Cretaceous palaeogeography of the northern Indian Plate margin. Detailed sedimentary logging, combined with geometrical analysis of large-scale, two-dimensional inclined exposures, is used to characterize and interpret the evolution of the fluvial succession. Variations in fluvial style and the controls upon them are discussed, along with the implications for the evolution of the Barmer Basin and its palaeogeographical setting in the early Cretaceous Period during the early separation of Indian Plate from Gondwana.

2 | GEOLOGICAL SETTING

The WIRS (Figure 1a) includes, from south to north, the Narmada, Cambay, Kachchh (Kutch), and Barmer basins (Akhtar & Ahmad, 1991; Biswas, 1987; Pandey, Fursich, & Sha, 2009; Rai, Singh, & Pandey, 2013). The formation of the WIRS was initiated in the mid to late Jurassic Period by the break-up of Gondwana as the eastern part, including the terranes of Greater India, Madagascar and Antarctica, separated from West Gondwana (Africa) in response to the development of the Mozambique and Somali proto-oceans west and north of Madagascar and India (Reeves, 2014; Reeves & De-Wit, 2000). Strike-slip reactivation of pre-existing Proterozoic structures (from tectonic inheritance: Misra & Mukherjee, 2015) in the Jurassic produced the Kachchh Basin (Biswas, 1982, 1999). By early Cretaceous times, development of the Mozambique and Somali proto-oceans gave way to sea floor spreading between the Greater Indian and Antarctic continents (Eagles & Hoang, 2014; fig. 3 of Bladon, Clarke, et al., 2015). Consequently, the northward movement and anticlockwise rotation of the Greater Indian continent occurred as break-up progressed (Chatterjee, Goswami, & Scotese, 2013; Storey et al., 1995; Torsvik et al., 2000) forming a series of interlinked failed rifts that constitute the WIRS. Although the Jaisalmer and Indus basins are well-known to have a late Gondwanan origin, the relationship between the Cretaceous sediments of the WIRS, the Jaisalmer and Indus basins remains obscure as it is patchily preserved across the northern margin of the Indian Plate below the Deccan Traps (Ahmad & Amad, 1991; Akhtar & Ahmad, 1991; Chowdhary, 1975; Jaitly & Ajane, 2013; Khosla et al., 2003; Misra & Mukherjee, 2015; Raju, 1968; Sharma, 2007; Sheth, 2007) and the geometry and extent of the associated rifts are poorly documented. That said, preservation of isolated fluvial Lower

Cretaceous sediments clearly suggests the presence of an established rift system through the north-western Indian Plate prior to the onset of the main Deccan eruptions around 64 Ma in the Danian (Mukherjee, Misra, Calvès, & Nemčok, 2017). Regional palaeogeographical reconstructions (Biswas, 1999; Chatterjee et al., 2013) also include continental rift basins between India, Madagascar, and the Seychelles microcontinent, although the geometry of these rifts and their sedimentary fills is very poorly described (see Plummer & Belle, 1995).

The Barmer and Cambay basins, together with the San-chor sub-Basin that separates them, form a present-day generally north-northwest trending rift “arm” of the WIRS extending up to 600 km into north-western India from the Gulf of Khambhat (Figure 1a). The Barmer Basin is a 200 km long, <40 km wide, 6 km deep, failed continental rift (Biswas, 1982; Bladon, Burley, et al., 2015; Compton, 2009; Dolson et al., 2015) (Figure 1b) containing continental sediments (Figure 2a; Compton, 2009; Dolson et al., 2015; Sisodia & Singh, 2000). A comparable rift system, generally known as the Thar or “Lower Indus” rift (Ahmad & Amad, 1991; Zaigham, Ahmad, & Hisam, 2012; Zaigham & Mallick, 2000) and specifically including the Panno-Aqil Graben, extends northwards into Pakistan south of the Mari-Kandkot High and east of the Jacobabad High (Ahmad & Amad, 1991) and probably represents the continuation of the WIRS (Figure 1a).

Subsidence and sedimentation along the WIRS presumably continued contemporaneously with rifting of the Seychelles microcontinent and eruption of the Deccan volcanics at the Cretaceous-Palaeogene boundary ~65 Ma (Collier et al., 2008; Eagles & Hoang, 2014; Ganerød et al., 2011; Plummer, Joseph, & Samson, 1998). The exact causes of this extension remain equivocal, with many authors citing the migration of the western margin of India over the Reunion Plume (Morgan, 1971; Plummer & Belle, 1995; Simonetti, Bell, & Viladkar, 1995), even though the present-day Reunion Plume impinges on a remnant of continental crust (Torsvik et al., 2013).

Post-Deccan subsidence was concentrated along the Cambay-Barmer rift where some 6 km of alluvial through to lacustrine environments of Palaeogene and Neogene age have accumulated (Roy & Jokhar, 2002; Sisodia & Singh, 2000; Tabaei & Singh, 2002; Tripathi, Kumar, & Srivastava, 2009). These sediments have developed under a tropical to sub-tropical climate (Ali & Aitchison, 2014; Chatterjee et al., 2013; Hallam, 1985) as the Indian Plate migrated northwards to its present-day position.

2.1 | The Barmer Basin

Rifting in the Barmer Basin resulted from two distinct non-coaxial extensional events (Bladon, Clarke, et al., 2015;

Dasgupta & Mukherjee, 2017). An earlier north-west to south-east extensional phase, oblique to the present orientation of the basin, was followed by dominantly Palaeogene north-east to south-west extension (Bladon, Clarke, et al., 2015). Together, these two rift events produced an asymmetrical half-graben in the north and a more symmetrical graben in the south. Seismic data from the Barmer Basin indicate that pre-Deccan rifting is present along the full extent of the basin with stratigraphical thickening being pronounced on the present-day eastern margin (Dolson et al., 2015).

Basement rocks of the Precambrian Malani Igneous Suite are unconformably overlain by clastic fluvial sediments of the Jurassic Lathi Formation and the Lower Cretaceous Ghaggar-Hakra Formation (Figure 2a). Eastwards the Ghaggar-Hakra Formation overlies the Karentia Volcanic Formation (Figure 2a), consisting predominantly of microcrystalline and plagioclase-phyric basalts (Roy & Jokhar, 2002) which erupted in response to initial rifting between east and west Gondwana (Bladon, Burley, et al., 2015; Reeves & De-Wit, 2000; Storey et al., 1995). Previous authors have ascribed all three of these formations to a “pre-rift succession” (Biswas, 1987; Compton, 2009; Roy & Jokhar, 2002).

Synrift strata are ascribed to the Palaeogene Mallinath Group and the early part of the Eocene Jagmal Group (Figure 2a). Earliest syn-rift strata of the Mallinath Group comprise acidic pyroclastics and basaltic lavas of the Raageshwari Volcanic Formation erupted predominantly in the centre of the basin (Compton, 2009), whilst contemporary alluvial fan sediments (the Dhandlawas Formation) were deposited along the western margin, adjacent to major fault scarps (Dolson et al., 2015). From Maastrichtian to Thanetian times, braid-plain fluvial and alluvial systems of the Fatehgarh and Barmer Hill formations dominated with alluvial fan deposition (Jogmaya Formation) along the western faulted margin and flanking horsts within. Regional uplift removed the youngest Barmer Hill strata to produce a widespread unconformity across the basin before deposition resumed in Ypresian times (Jagmal Group). Lacustrine systems (Dharvi Dugar Formation) dominated during the early Jagmal Group giving way to swamp clastics of the Thumbli and Akli formations by Lutetian times exhibiting minor marine incursions.

Post-rift subsidence and in-fill began in Lutetian times with lacustrine sediments of the Nagarka Formation (Dolson et al., 2015). A period of uplift coincided with collision of the Indian and Eurasian plates developed the regional base Miocene unconformity, before deposition of the fluvial and alluvial Neogene Jagadia and Uttarlia formations of the Rawal-Umed Group (Najman et al., 2018).

2.2 | The Ghaggar-Hakra Formation

In the Sarnoo Hills, a succession of fluvial sediments unconformably overlay volcanic rocks of the Karentia Volcanic Formation and, in places, the Malani Igneous Suite (Figure 2b; Baksi & Naskar, 1981; Compton, 2009; Mishra et al., 1993; Sisodia & Singh, 2000). The formation is ~100 m thick at outcrop (Mishra et al., 1993) and comprises three distinct, quartz-rich, fluvial channel belt sandstone packages separated by ~30 m of variegated white and red coloured, horizontally laminated and cross-laminated sands, with rhizoliths and soft-sediment deformation structures (Bladon, Burley, et al., 2015), attributed to deposition on a fluvial floodplain (Bladon, Burley, et al., 2015; Bladon, Clarke, et al., 2015). The sandstone packages have been assigned informal lithostratigraphical status and named (in ascending order): the Darjaniyon-ki Dhani, Sarnoo and Nosar sandstones (Figure 2b; Bladon, Burley, et al., 2015; Bladon, Clarke, et al., 2015).

The Darjaniyon-ki Dhani Sandstone comprises poorly sorted and clast-supported lithic arenites along with coarse sand to pebble-grade conglomerates attributed to deposition in an immature, braided system with a high sediment load (Bladon, Burley, et al., 2015). The Sarnoo Sandstone comprises cyclic, well-sorted, fine to medium-grained, quartz arenites with regular cross-bedded sets (Sisodia & Singh, 2000) and deposited in a mobile meandering system (Bladon, Burley, et al., 2015). The Nosar Sandstone caps the formation at outcrop and comprises medium to coarse-grained sands and granule-grade conglomerates with cross-bedded sets and channel geometries with erosive bases, typical of deposition in an actively migrating braided fluvial system (Bladon, Burley, et al., 2015).

Plant leaves (*Phlebopteris athgarhensis* Jain, *Ptilophyllum acutifolium* Morris and ?*Sphenopteris* sp.; Baksi & Naskar, 1981; Compton, 2009; Rajanikath & Chinnappa, 2016) are present within the formation and are characteristic of the *Dictyozamites-Pterophllum-Anomozamites* Assemblage (eighth) zone (Dev, 1987; Rajanikath & Chinnappa, 2016). Together with trisaccate pollen (*Podocarp Microcachrydites* spp., *Cyclusphaera* spp.), they date the Ghaggar-Hakra Formation to the Lower Cretaceous Epoch. Further constraints on the earliest age of the formation are provided by an Aptian (120 Ma) date for the underlying basalts of the Karentia Volcanic Formation (Sharma, 2007) and basaltic intrusions of Deccan age (68.57 ± 0.08 Ma; Basu, Renne, DasGupta, Teichman, & Poreda, 1993) constrain the youngest age of these sediments, indicating the formation is Aptian to Albian age.

3 | DATASET, METHODS, AND FIELD AREA

The Ghaggar-Hakra Formation is exposed in a series of three low-lying, fault-bounded hills separated by a peneplained surface covered in modern desert deposits near the village of Sarnoo. Progressive down-stepping of the faulted blocks towards the west and north provides excellent exposures that can be correlated providing continuous, composite vertical sections. Extensive quarrying provides continuous lateral exposure of the sediments in the scarp slopes of these hills. The dataset consists of 114 detailed sedimentary logs (Figure 3) and 53 detailed two-dimensional panels providing correlation and geometries between the logs.

3.1 | Sedimentology of the Ghaggar-Hakra Formation

The details of lithofacies are given in Table 1 and Figure 3. Eight architectural elements (Table 2 and Figures 4–6) are

identified and summarized below with the bounding surface terminology of Miall (1985, 1988).

3.1.1 | Channel element—Ch

Description

These “U”-shaped elements (Table 2)—laterally up to ~25 m and ~7 m thick—are bound by sharp, sometimes erosional, convex-down fifth-order surfaces at their bases, and generally planar and concordant fourth-order surfaces at their tops. The basal fifth order bounding surface erodes other elements of this type (Ch), overbank (Ob), or channel margin (Cm) elements but the fourth order surface, where preserved, is gradational over approximately 2 m into overlying point bar (Pb) or overbank (Ob) elements. Typically, the full geometry is not preserved, eroded by younger channels (Ch), channel margins (Cm), gravel bars (Gb), point bars (Pb), or sheet flows (Sf; Figures 4a, 5a and 6a).

The fifth order surface is immediately overlain by the pebble-grade quartz clasts of grain-supported conglomerate (G) characterized by indistinct cross-bedding. The

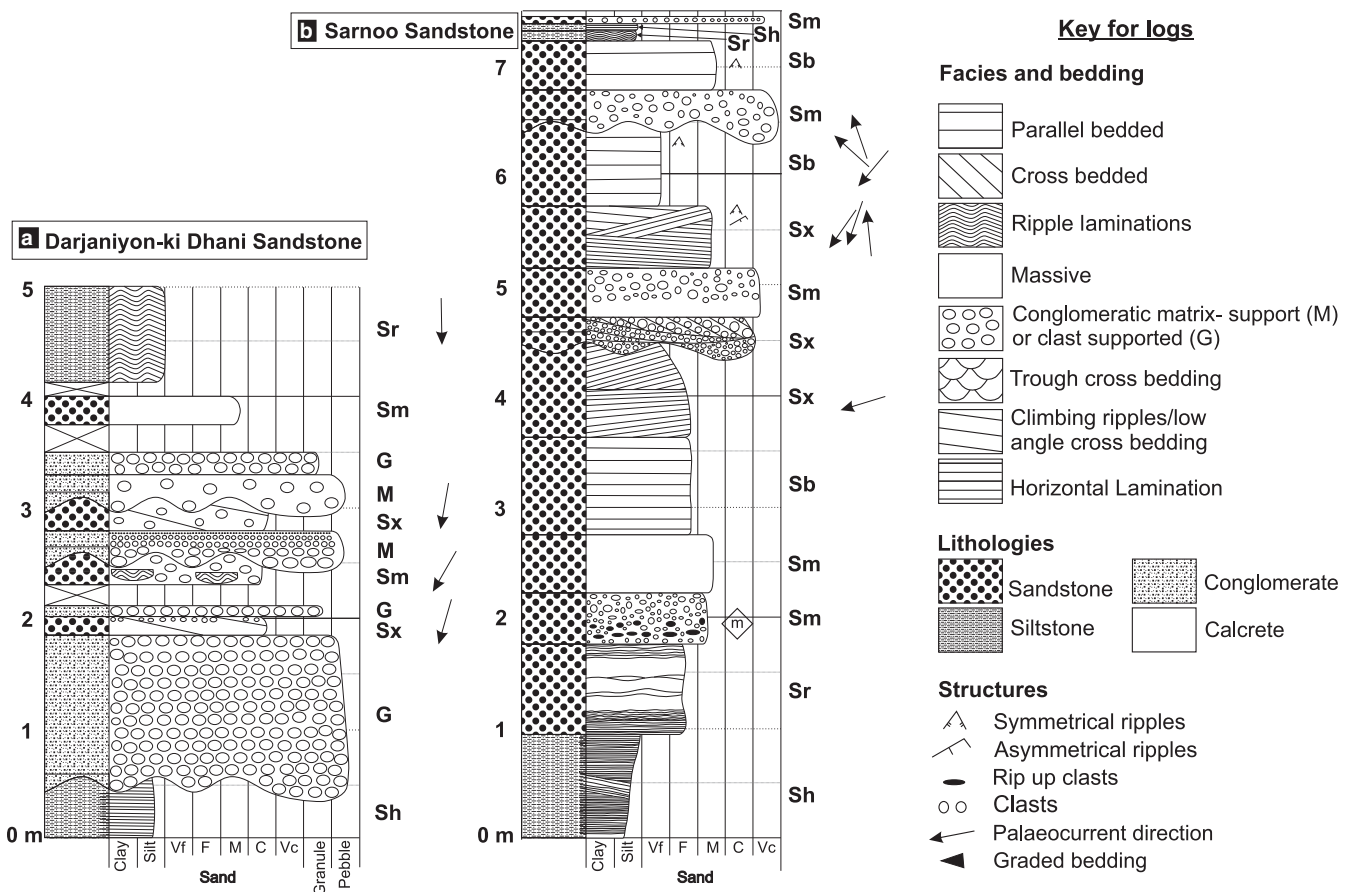




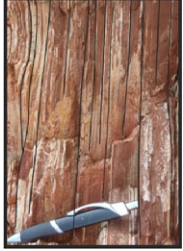

FIGURE 3 Simplified representative logs from the Ghaggar-Hakra Formation. Three logs displaying the typical facies from (a) the Darjaniyon-ki Dhani Sandstone, (b) the Sarnoo Sandstone, and (c) the Nosar Sandstone. The facies codes stated on the logs are denoted in Table 1, the arrows represent the palaeoflow orientation and logs are in metres

TABLE 1 Fluid, debris, and subaerial facies of the Ghaggar-Hakra Formation developed from the logged and panelled data of the formation

Lithofacies	Texture	Structures	Interpretation	GPS location	Figure
Fluid flow facies					
G (clast-supported conglomerate)	Sub-rounded pebble-grade quartz and lithic clasts (2–52 mm), poorly sorted	Erosional surfaces, grading of the clasts and indistinct cross-beds	Confined lower flow regime, potential migration of dune-scale bedforms	UTM 0777247, 2841083	
Six (Trough cross-bedded sandstone)	Fine- to coarse-grained sands, moderately sorted, sub-rounded with rounded pebbles of quartz (22 mm)	Trough cross-bedding and erosional surfaces	Migration of sinuous crested dune-scale bedforms in the lower flow regime	UTM 0778735, 2842021	
Sx (Planar cross-bedded sandstone)	Fine- to coarse-grained, well-sorted, sub-rounded, with rounded pebbles of quartz (50 mm)	Planar cross-bedding, u-shape structures, reactivation and erosional surfaces	Migration of straight crested dune-scale bedforms in the lower flow regime	UTM 0782621, 2853326	
Sb (Parallel-bedded sandstone)	Very fine- to coarse-grained, moderately sorted, sub-rounded, clasts (22 mm)	Parallel bedding, erosional surfaces, silt bands, with very occasional cross-beds	Non- or partially confined flow events with bedload-dominant transport and sporadic dune bedforms	UTM 0782621, 2853326	
Sla (low-angle cross-bedded sandstone)	Fine- to coarse-grained sands, moderately sorted, sub-rounded	Low-angle cross-bedding	Sediments likely deposited due to helical flow during lateral migration	UTM 0777898, 2840794	

(Continues)

TABLE 1 (Continued)

Lithofacies	Texture	Structures	Interpretation	GPS location	Figure
Sr (Rippled sandstone)	Very fine- to medium-grained, well-sorted, sub-rounded	Symmetrical and asymmetrical ripples upon laminated and bedded sediments	Ripple-scale bedforms in the lower flow regime	UTM 0777801, 2841812	
Srha (Rippled sandstone with super-critical climbing)	Very fine- to medium-grained, well-sorted, sub-rounded	Fully preserved symmetrical and asymmetrical ripples	Ripple-scale bedforms in the lower flow regime; high sediment output		
Scl (Cross-lamination sandstone)	Fine-grained sands, well-sorted, sub-angular	Cross-lamination	Ripple-scale bedforms in the lower flow regime	UTM 0783859, 2853121	
Sh (Horizontally laminated)	Fine- to medium-grained sands, moderately sorted, sub-angular	Laminations	Low amplitude, long wavelength bedforms of the upper flow regime	UTM 0783727, 2853017	
Sm (Massive sandstone)	Fine- to coarse-grained, on occasion there are clasts up to 19 mm	Massive	Material deposition from suspension, in very low slow moving or stationary waters	UTM 0777107, 2840577	
Im (Massive siltstone)	Siltstone	Massive	Material deposition from suspension, in stationary waters	UTM 0777181, 2841039	

(Continues)

TABLE 1 (Continued)


Lithofacies	Texture	Structures	Interpretation	GPS location	Figure
Debris flow facies					
M (Matrix-supported conglomerate)	<27 cm boulders, where the matrix is granule-grade conglomerates; the material is matrix-supported	Indistinct cross-bedding	Non-Newtonian flow resulting from high sediment load suppression of bedforms	UTM 0777865, 2841891	
Subaerial facies					
Sp (Pedogenic sandstone)	Mottled red and white very fine-grained sands	Occasional laminations, soft-sediment deformation and indistinct bedding and laminations	Bioturbation from plants and organisms and a pedogenic nature equalling soil formation	UTM 0778635, 2842386	
Ip (Pedogenic siltstone)	Mottled red and white, muds and silts	Occasional laminations, soft-sediment deformation, and indistinct bedding and laminations	Pedogenic nature, soil slickenlines, fractures, and bioturbation from root traces and organisms allowing for soil formation	UTM 0778640, 2842381	
Ihe (Haematitic siltstone)	Mottled red and white, muds and silts	Haematitic horizons with occasional laminations, soft-sediment deformation and indistinct bedding and laminations	Bioturbation from plants and organisms, haematitic and a pedogenic nature equalling soil formation	UTM 0778635, 2842386	

TABLE 2 Architectural elements of the Ghaggar-Hakra formation

AE	Lithofacies	Description	Interpretation
Ch	G, Stx, Sx, Scl, Sh, Sp	<i>Geometry:</i> Tabular and sheet-like geometries <i>Size:</i> up to 6 m thick <i>External boundaries:</i> Lower fifth-order surfaces are erosional and the upper fourth boundaries are gradational where seen <i>Internal boundaries:</i> First- to third-order bounding surfaces	Packages of sediment represent in-channel deposits
Cm	Sx, Sh, Scl, Sp, Ip	<i>Geometry:</i> Wedged and tabular <i>Size:</i> Up to 5 m thick and 10 wide <i>External boundaries:</i> Lower fifth order surface is sharp and the upper fourth order surface is gradational <i>Internal boundaries:</i> First- to third-order bounding surfaces	Deposited due to flow migrating from a confined to an unconfined setting
Gb	G, M, Sm, Sh	<i>Geometry:</i> Lenticular to wedge-shaped <i>Size:</i> <6 m high and 300 m in lateral extension <i>External boundaries:</i> Lower fifth order boundaries are erosion and the upper fourth order boundaries are gradational <i>Internal boundaries:</i> First- to third-order surfaces	Transient braid bars, with deposition by migrating bedforms
Cc	G, Sm, Im, Sh, Sp, Ip	<i>Geometry:</i> Lenticular and wedged shaped <i>Size:</i> Channels are <70 cm in height and 2 m wide <i>External boundaries:</i> Lower fifth order boundaries are erosional and the upper fourth order boundaries are gradational <i>Internal boundaries:</i> No internal bounding surfaces, generally structureless, can contain normal grading	Flooding of the river system by cutting off the point bar
Pb	Sla, Sx, Scl	<i>Geometry:</i> Wedge <i>Size:</i> <3 m in height, and 20 m in length <i>External boundaries:</i> Lower order fifth order bounding surface and the fourth order bounding surface are gradational <i>Internal boundaries:</i> First and second order bounding surface which truncate against third- and fourth-order bounding surfaces where the sets and cosets are perpendicular to one another	Laterally migrating bars
Sf	Sr, Sh, Srha, Sb, Scl, Sp, Ip	<i>Geometry:</i> Sheet-like and tabular <i>Size:</i> laterally extensive (<2 km) and 2 m high <i>External boundaries:</i> Lower fifth order bounding surface is concave-down and concordant and the upper fourth order bounding surface is gradational <i>Internal boundaries:</i> Interbedded laminations and ripples with first- and second-order bounding surfaces	Formed through the flooding of the fluvial system
Ob	Sh, Sm, Im, Sr, Scl, Sp, Ip, Ihe	<i>Geometry:</i> Tabular and sheet-like <i>Size:</i> Up to 150 cm in thickness and 2 km in lateral extension <i>External boundaries:</i> Lower fourth-order bounding surface is sharp and the upper fourth order bounding surface is sharp <i>Internal boundaries:</i> First- to fifth-order surfaces are present; the first- to third-order surfaces are from ripples, fourth-order surfaces are sharp and form from the pond element. The fifth-order surfaces are regional quiescence periods	Formed from cyclic flooding from the fluvial system, with palaeosol evident
Po	Scl, Sm, Im, Sr, Sh, Ip, Ihe	<i>Geometry:</i> Sheet-like and tabular <i>Size:</i> <0.5 m high and 20 m in length <i>External boundaries:</i> both the lower and upper fourth order boundaries are gradational into the floodplain element <i>Internal boundaries:</i> First- and second-order surfaces present with boundaries removed due to bioturbation	Slight coarsening upwards successions, capped with palaeosols

channel elements and become erosional. Sporadically, basal surfaces are replaced by a slightly gradational contact from the underlying channel elements (Ch). Upper fourth-order surfaces are sharp with the overlying sediments of gravel

bar (Gb), point bar (Pb), sheet flow (Sf), or overbank (Ob) elements.

Bases are overlain by stacked, sub-critically climbing sets (30 cm) and cosets (95 cm) of planar cross-bedded

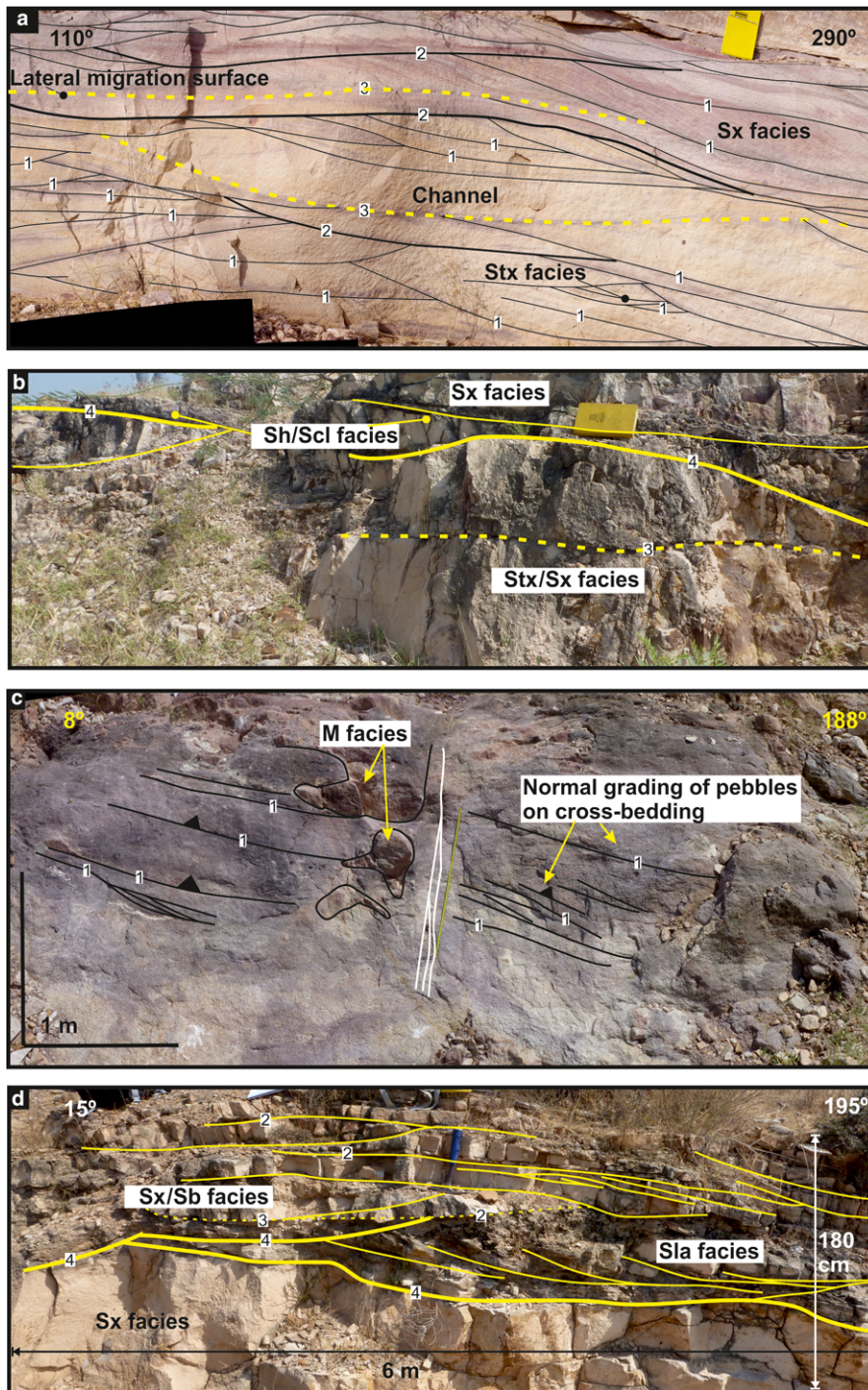


FIGURE 4 Interpreted photographs of the architectural elements (a) Channel element (Ch) displaying first- to third-order bounding surfaces with the trough and planar cross-bedded sandstone facies; (b) Channel margin element (Cm) displaying the gradational change from the cross-bedded facies (Stx/Sx) into the cross/horizontal-lamination facies (Sh/Scl) overlain by an erosional surface and the planar cross-bedded facies; (c) Gravel bar element (Gb) displaying the conglomerate facies (M & G) with indistinct cross-bedding and upon some of the cross-beds there are graded clasts; (d) Chute channel element (Cc) this image depicts the channel element indicated by the planar cross-bedded facies (Sx), the Point bar element indicated by the low-angle cross-bedded facies (Sla) and the chute channel indicated by the thick, thin solid lines and the planar cross-bedded and planar horizontally bedded facies (Sx/Sb); (e) Point bar element (Pb) with low-angle cross-bedded facies (Sla) with second- and fourth-order bounding surfaces laterally migrating into the channel element (Ch); (f) Sheet flow element (Sf), here the element displays the horizontal-laminated and cross-lamination facies (Sh/Scl) with various types of ripples; (g) Overbank element (Ob) indicated by the rhizoliths and the pedogenic facies (Sp/Ip/Ihe), and; (h) Pond element (Po) indicated by the horizontal-laminated and cross-lamination facies (Sh/Scl)

sandstone (Sx) bounded by first- to third-order surfaces. Above these, sets of cross-laminated sandstone (Scl) climb sub-critically at 5° . Capping the elements are deposits of fine-grained, horizontally laminated sandstone (Sh), and pedogenic facies (Sp, Ip; Figures 4b, 5b and 6b).

Interpretation

These elements are interpreted as representing the deposition of sediments on the channel margin as flooding occurs. Sets of cross-bedded sandstone (Sx) and cross-laminated

sandstone (Scl) represent the development and migration of dune- and ripple-scale bedforms as the flow overtops the channel on to the floodplain and wanes (O'Conner, Jones, & Haluska, 2003; Wakefield, Hough, & Peatfield, 2015). The presence of horizontally laminated sandstone suggests periodic episodes of upper flow regime conditions as water moves from the restricted channel to an unrestricted floodplain (Brierley, Fergusin, & Woolfe, 1997). Mottled sands and silts with poorly preserved bedding possibly indicate destruction of primary depositional fabrics by vegetation.

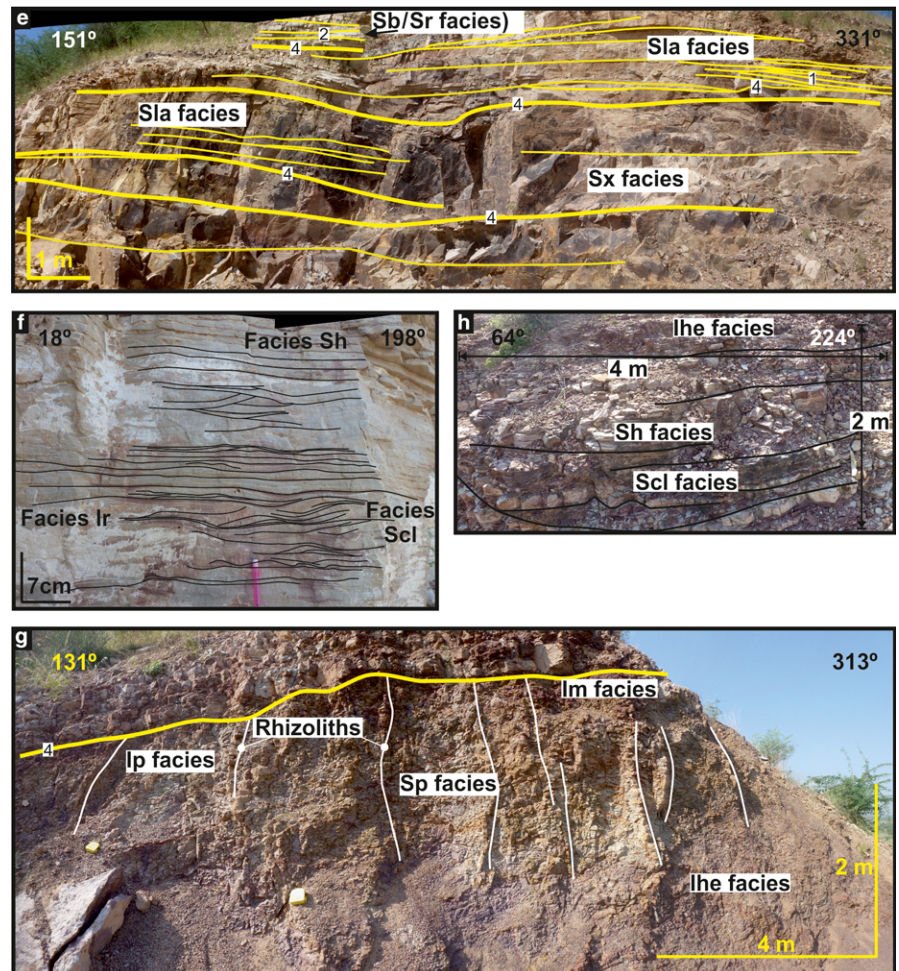


FIGURE 4 Continued

3.1.3 | Gravel bar element—Gb

Description

These lenticular elements—up to 75 m long and 4 m thick—are bound by sharp and erosive fifth-order surfaces at their bases, eroding into channel (Ch) or overbank (Ob) elements, and sharp or gradational fourth-order surfaces into the channel, point bar, or overbank elements (Ch, Pb, Ob; Figures 4c, 5c and 6c, Table 2). Fifth-order surfaces are laterally extensive and can transition laterally into fifth-order surfaces at the base of channel elements (Ch).

Matrix-supported conglomerates (M) and/or clast-supported conglomerates (G) immediately overly the bases. Matrix-supported conglomerates (M) comprise rounded quartz clasts and extraformational lithics, supported in a matrix of very fine to fine-grained sandstone. Sporadically, indistinct foresets of cross-bedding are present. Clast-supported conglomerates (G) comprise poorly sorted but rounded pebbles of quartz and extraformational lithic clasts with sporadic and indistinct cross-beds.

The upper third comprises either massive sandstone (Sm) or horizontally laminated sandstone (Sh) facies (Figure 6c), exhibiting sharp contacts with the underlying

sediments. The massive sandstone is moderately to poorly sorted with numerous quartz clasts. The clasts are typically distributed randomly, but sporadically form indistinct horizontal layers. The horizontally laminated sands are up to 9 mm thick but thin upwards. The full succession is rarely preserved and conglomerates (M, G) dominate.

Interpretation

Highly erosional fifth-order surfaces typically contiguous with those of channels and conglomeratic sediments indicate gravel bar deposition primarily by bedload transport under high-energy conditions (Froude et al., 2017). This deposition is likely to have occurred along the bases of developing channels with long axes of bars parallel to the channel. Grain size is not conducive to producing bedforms, and a high sediment load promotes rapid deposition that further suppresses their development (Bridge & Best, 1988). Where sediment load is reduced, deposits grade from matrix to clast-supported with sporadic and poorly developed cross-bedding indicating some migrating bedforms (Blair & McPherson, 1994) and implying transient gravel bar movement (Figures 4c, 5c and 6c; cf Bridge, 1993).

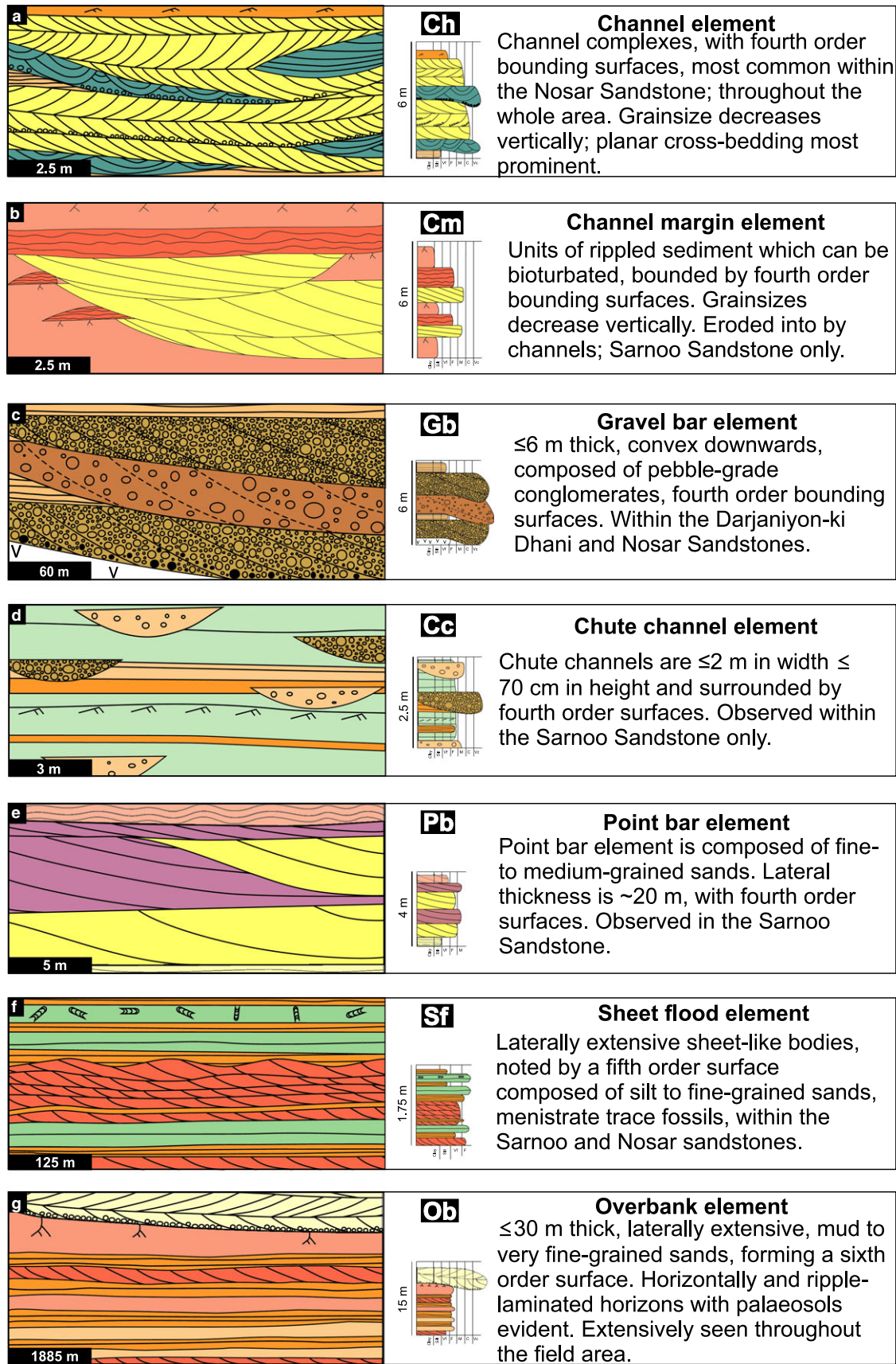


FIGURE 5 Two-dimensional sketches and logs that typify the architectural elements observed in the Ghaggar-Hakra Formation (a) Channel, Ch; (b) Channel margin, Cm; (c) Gravel bar, Gb; (d) Chute channel, Cc; (e) Point bar, Pb; (f) Sheet flow, Sf; (g) Overbank, Ob, and; (h) Pond, Po

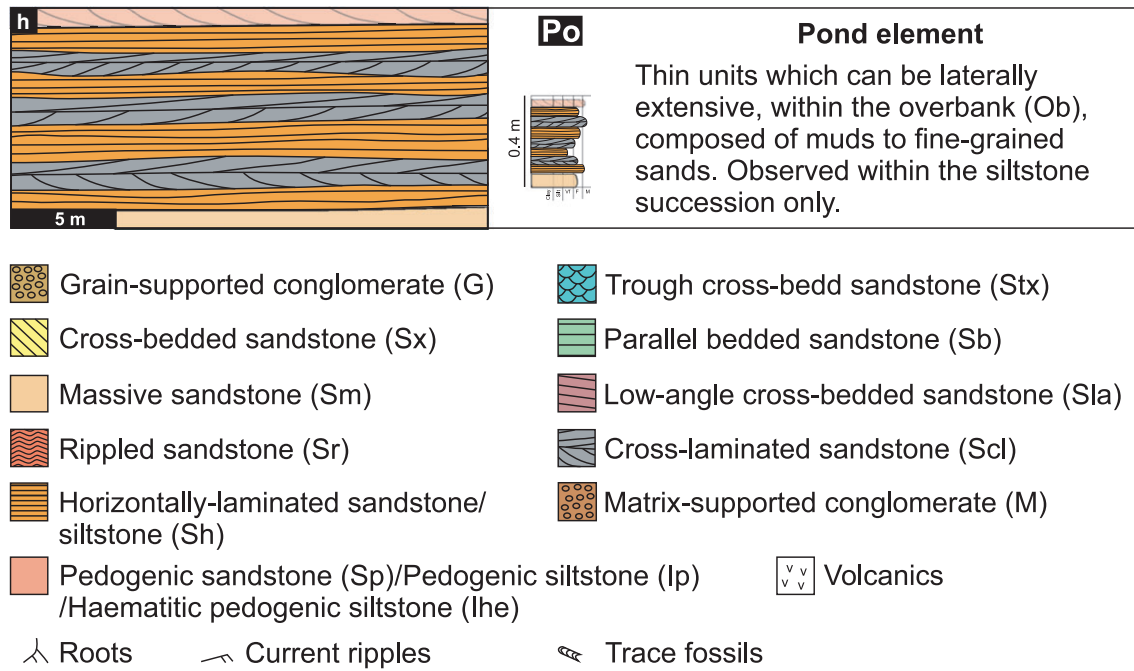


FIGURE 5 Continued

Massive and horizontally laminated sandstone represents deposition in shallow water on top of the developing bar-forms. Horizontally laminated sandstone was deposited under upper flow regime conditions (Ghazi & Mountney, 2009) when the gravel bars were fully submerged. Massive sandstone represents deposition when the top of the bar was at surface or slightly emergent, and stationary waters allow suspension fall out (Banham & Mountney, 2013; Jones & Rust, 1982).

3.1.4 | Chute channel element—Cc

Description

These small, symmetrical “U”-shaped elements are up to 70 cm in height and no more than 2 m wide (Table 2). Their lower fifth-order bounding surfaces are convex-down and erosional into either point bar (Pb) or overbank (Ob) elements. Upper fourth-order surfaces are generally gradational into the overbank elements (Ob) over a thickness of 50 cm (Figures 4d, 5d and 6d).

Internally, the succession fines upwards from grain-supported conglomerates (G) composed of quartz clasts, through massive sands and silts (Sm, Im) containing quartz clasts up to 5 mm. This succession culminates in parallel-bedded sands and silts forming ~50 cm thick packages with individual beds ranging between 10 and 15 cm thick and the horizontally laminated sandstone (Sh) with packages up to 80 mm with laminations up to 9 mm thick. Capping this element are bioturbated, rooted, pedogenically modified fine-grained sands and silts (Sp, Ip). Typically, the succession is fully preserved, but sporadically, granule-grade conglomerates (G) pass

straight into pedogenically modified sands and silts (Sp/lp) producing a strongly bimodal grain-size profile.

Interpretation

The “U”-shaped geometries and their erosional lower bounding surfaces are indicative of small-scale channels. Conglomerates (G) consisting of locally reworked material immediately overlying fifth-order surfaces suggest initial deposition of sediments in a high-energy flow cutting channels (Bordy, Hancox, & Rubidge, 2004). Subsequently, flow waned rapidly to stagnant conditions with a high sediment load promoting deposition of massive sands and silts (Sm, Im; Martin & Turner, 1998). Where present, parallel-bedded and horizontally laminated sandstone (Sb, Sh) may suggest periods of extended and fluctuating upper flow regime conditions prior to rapid waning (Wakefield et al., 2015). In other examples, flow waned rapidly to stagnant water, depositing a strongly bimodal grainsize (Martin & Turner, 1998).

The strong spatial association between these elements and point bar elements (Pb), coupled with palaeocurrents that are generally perpendicular to the main channel system, suggests small-scale, high-energy chute channels formed during flood conditions (Ghinassi, 2010; Wakefield et al., 2015). During flooding, sediment load is high, increased discharge promotes “short-cutting” of the system across meanders, and energy levels wane rapidly to promote rapid and structureless deposition (Wakefield et al., 2015). Further evidence for this interpretation is provided by the presence of locally reworked quartz clasts most likely derived directly from the main channel system. Pedogenic sands and silts (Sp, Ip) represent bioturbation and reworking of later

stage sedimentation. The geometries of these elements suggest “low sinuosity” chute channels comparable to the “type 1” chute channel of Ghinassi (2010).

3.1.5 | Point bar element—Pb

Description

These wedge-shaped elements (Table 2), up to 4 m thick and a maximum of 15 m wide, are bound by lower fifth-

order surfaces that are sporadically slightly erosional but are generally concordant with underlying strata and typically extend laterally into the base of a channel (Ch). Upper fourth-order surfaces, where preserved, are concordant with sediments of overbank (Ob) and/or channel margin (Cm) elements. Typically, the upper parts of these elements are not preserved because of erosional down-cutting by chute channel (Cc), channel (Ch) or sheet flow (Sf) elements (Figures 4e, 5e and 6e).

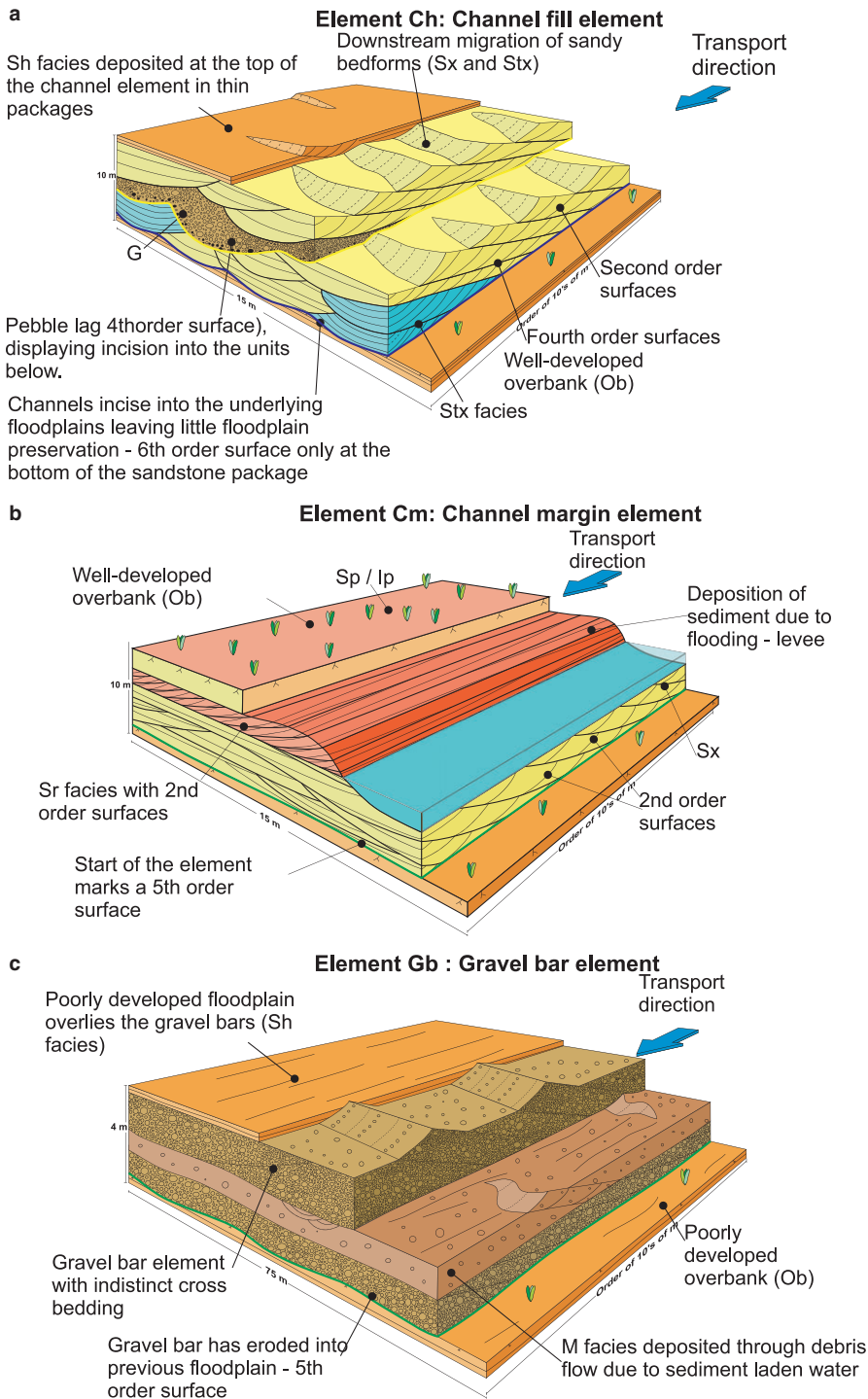


FIGURE 6 Three-dimensional facies models of the architectural elements. (a) The channel element (Ch) with an erosive lower base contains first- to third-order surfaces internally. (b) The channel margin (Cm) element with an erosive lower base and first- to third-order surfaces internally, the succession grades into the overbank. (c) The gravel bar (Gb) element with an erosive lower boundary and first- to second-order surfaces within. (d) The chute channel (Cc) element with an erosive lower boundary and occasional first order boundaries within. (e) The point bar (Pb) element with an erosive fourth order boundary with first- to third-order surfaces internally. This succession grades into the overbank. (f) The sheet flow (Sf) element starting with a lower fourth order bounding surface with first- to third-order surfaces within. There are quiescent periods here evidenced by trace fossils. (g) The overbank (Ob) element with first, second, and fourth-order surfaces within. (h) The pond (Po) element has a fourth order base and first- to second-order surfaces internally

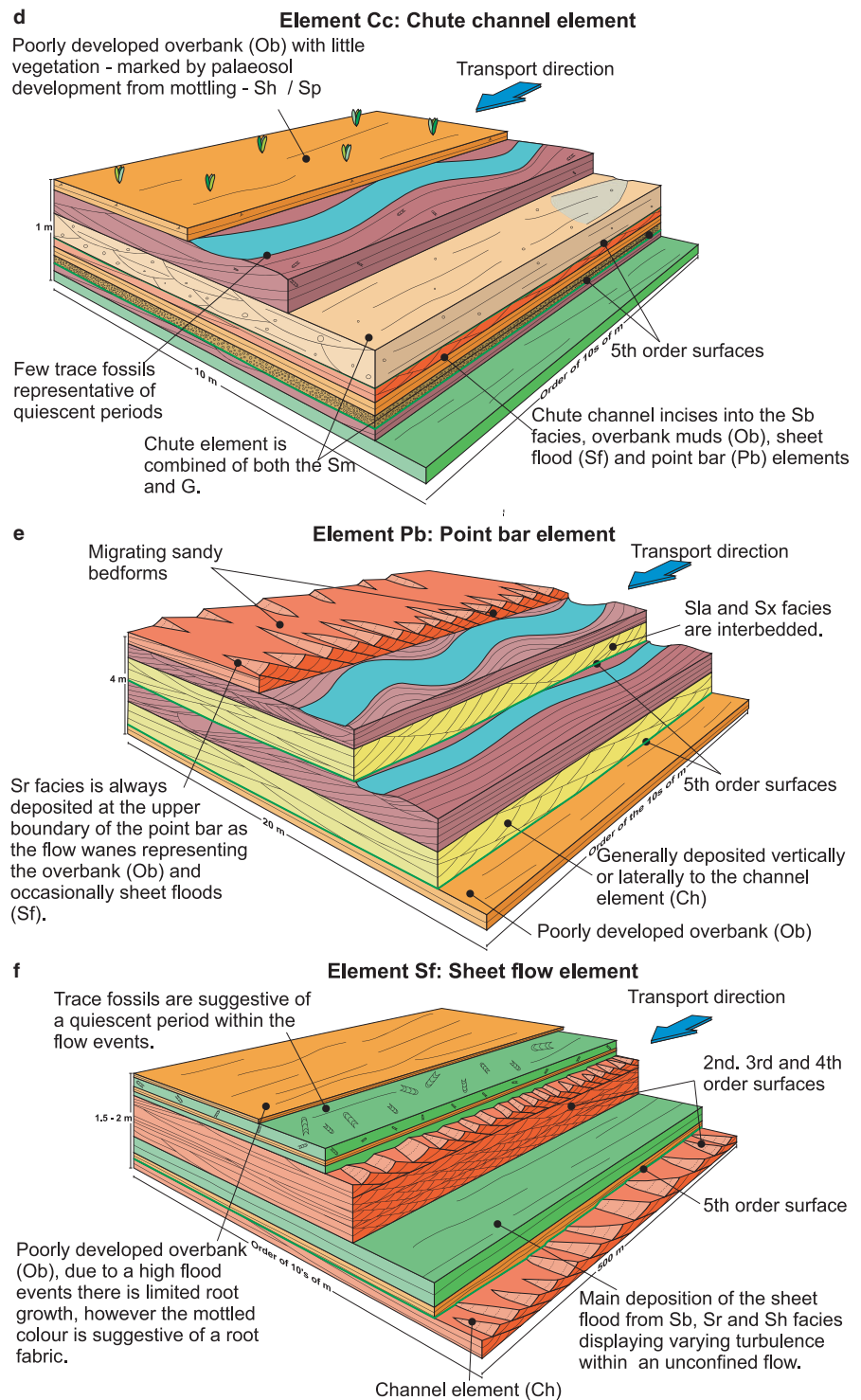


FIGURE 6 Continued

Overlying the fifth-order surfaces are cosets (95 cm thick) of planar cross-bedded sandstone (Sx) comprising sets of up to 30 cm thick that are interbedded with 2 m thick cosets of low-angle cross-bedded sandstone (Sla). This succession generally fines upward. Sets of both facies are bound by first- or second-order surfaces and sporadically truncated by third-order surfaces. Capping the elements is cross-laminated sandstone (Scl) forming individual

sets up to 5 cm thick with internal structures disrupted by miniscate trace fossils of *Taenidium* or *Beaconites* (Gowland, Taylor, & Martinus, 2018).

Interpretation

Elements of this type are interpreted as representing the deposits of laterally accreting point bars. Multiple sets and cosets of cross-strata decreasing in size from dune to ripple-

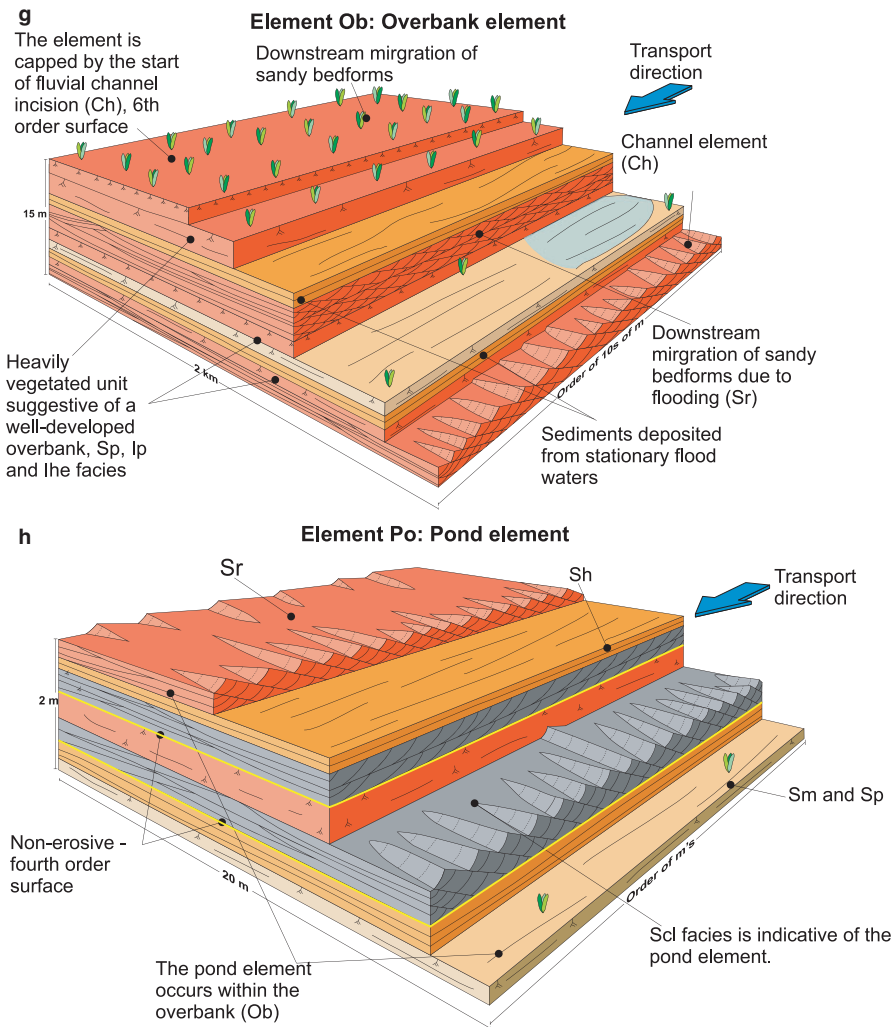


FIGURE 6 Continued

scale (Sx, Sla, Scl) are the product of migrating bedforms within the lower flow regime (Ghazi & Mountney, 2009; Jackson, 1976), this, combined with the reduction of grain-size indicates a waning flow. The complex and varied geometry of sets and cosets and numerous bounding surfaces of varying scales suggest dominantly lateral but slightly downstream migrating bedforms. Third-order surfaces suggest frequent reactivation and meniscate trace fossils towards the top suggest calm, possibly emergent, conditions with ripple-lamination representing wash-over of the bar (Bridge, Alexander, Collier, Gawthorpe, & Jarvis, 1995). Fifth-order bounding surfaces grading laterally into the bases of channel elements (Ch) and the spatial association of these two elements demonstrate an evolutionary relationship between them suggesting attachment of the bar to the channel.

3.1.6 | Sheet flow element—Sf

Description

These sheet-like tabular elements (Table 2), with a thickness of ~0.5 m, are bound by lower fifth-order surfaces that are convex-down and erosive. Where the elements are fully

preserved, fourth-order surfaces bound their tops and separate them from the overlying overbank (Ob) elements. However, the tops of the elements are typically marked by erosive surfaces at the bases of successive elements of sheet flow (Sf), or at the bases of channel (Ch), chute channel (Cc) or point bar (Pb) elements (Figures 4f, 5f and 6f).

Facies of these elements form an ordered succession. Beds up to 30 cm thick of parallel-bedded sandstone (Sb) fine and thin upward into beds of horizontally laminated sandstone (Sh). Overlying these are sets (10 cm) of rippled sandstone (Srha), climbing super-critically up to 30°, and stacked 30 cm cosets of cross-laminated sandstone (Scl) climbing sub-critically at 5°. Pedogenic sandstone and siltstone (Sp, Ip) display mottled textures, and contain fossil leaf imprints along with meniscate trace fossils typical of *Taenidium* or *Beaconites* (Gowland et al., 2018).

Interpretation

Deposition of subaqueous facies above fifth-order surfaces with sheet-like geometries indicates a largely unconfined flow (Blair, 2000). Upper flow regime conditions initially prevailed, depositing parallel-bedded sandstone and horizontally

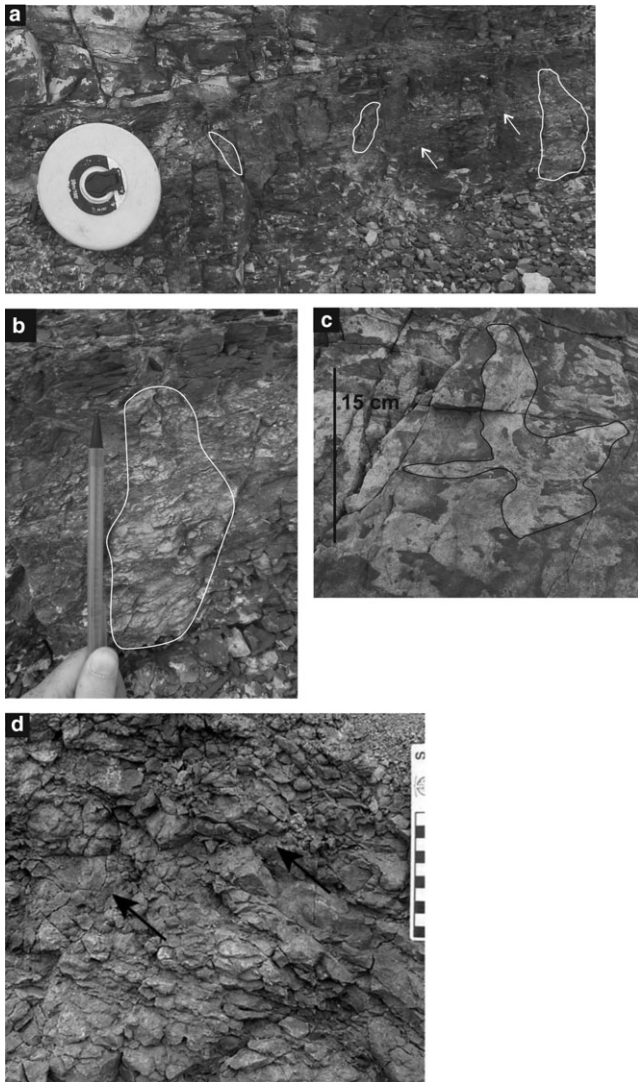


FIGURE 7 Rhizoliths within the floodplain (Ob) sediments (a) and (b) orange rhizoliths within the formation; (c) white reduction zones due to the organic material within the roots and rhizoliths, and; (d) the orange rhizoliths from Kraus and Hasiotis (2006), to allow for an easy comparison

laminated sandstone (Sb, Sh). Waning occurred rapidly to lower flow regime conditions depositing rippled sandstones (Srha, Scl; Hjellbakk, 1997) indicating bedform development and migration. Variations in climbing angle suggest variations in sediment load, flow competency, and capacity (Blair, 2000; Hampton & Horton, 2007; Hunter, 1977a, 1977b). Pedogenic facies with high levels of bioturbation and abundant plant remains implies times of depositional quiescence (Bromley & Asgaard, 1979, 1991; Buatois & Mangano, 2002).

The relationships between sheet flows, channels, and bars (Sf, Ch, Pb, and Gb) suggest that, whilst largely “unconfined” (Banham & Mountney, 2013), the sheet flows may be restricted to the lateral extent of active channel belts and most probably represent times of high discharge when channels were filled to capacity.

3.1.7 | Overbank element—Ob

Description

These elements are dominantly tabular (Table 2), up to 1.5 m thick and 2 km in lateral extent and bound at their tops and bottoms by planar fourth-order surfaces except where tops are eroded by overlying channel (Ch) or gravel bar (Gb) elements. Lower boundaries can be sharp where overbank elements overlay gravel bars (Gb), or gradational where they overlay point bar or sheet flood (Pb, Sh) elements (Figures 4g, 5g and 6g).

The facies occur in any order, but when massive sandstone and siltstone (Sm, Im) and/or horizontally laminated sandstone (Sh) are present they typically overlay the fourth order surface, interbedded in an apparently random manner by individual sets of cross-laminated sandstone (Scl). When present, together these facies account for no more than 15% of the element with the remainder comprising pedogenic facies (Sp, Ip, Ihe). Pedogenic facies are dominantly red, and contain abundant granular pedes (Retallack, 1988) between 2 and 3 cm long, along with grey to white patches of generally coarser grain. Abundant orange goethite-rich rhizoliths reach lengths of 15 cm (Figure 7), and carbonate-cemented rhizoliths reach lengths of 1 m (Figure 4g) along one particular horizon. All facies are remarkably fissile, and rare root structures and soils slickensides can be found throughout.

Interpretation

The physical dimensions and particularly the lateral extents indicate sediments of unconfined overbank floods. The facies indicate sub-aqueous upper (Sh Sm) and lower flow regime conditions with limited bedform development or migration (Scl) and occasional suspension settlement (Sm, Im). Facies displaying granular pedes and extensive colour mottling indicate significant bioturbation (Sp, Ip, Ihe; Retallack, 1988; Tennvassås, 2018), subaerial exposure, and palaeosol formation (Retallack, 1988, 1990).

Elements of this type typically overlie one another, with little to no erosion, and likely represent cumulative soil growth on a floodplain supplied regularly with sediment from flooding (Kraus, 1999; Kraus & Aslan, 1999). The rhizoliths indicate floodplain areas were imperfectly to poorly drained soils (Kraus & Hasiotis, 2006) suggesting they were seasonally wet (Retallack, 1990).

3.1.8 | Pond element—Po

Description

These elements form lenticular bodies—up to 2 m thick and 50 m wide (Table 2). The lower and upper boundaries are both fourth-order surfaces and this element grades into the overbank (Ob) element over ~30 cm.

Facies do not form regular definable successions, but where present cross and horizontally laminated sandstones (Scl, Sh) are typically preserved near element bases, followed by massive fine-grained sandstone and siltstone (Sm, lm), with pedogenic (Ip) and haematitic siltstone (lhe) dominating.

Interpretation

Elements of this type are interpreted as small ponds of limited lateral extent developed on the overbank areas. Horizontally laminated sandstone, massive sandstone, and massive siltstone (Sh, Sm, lm) indicate that sediment deposition was dominated by suspension settlement. Sporadic cross-lamination (Scl) indicates development and migration of small ripple-scale bedforms when pond levels were recharged by overbank flooding. Wind shear on standing water combined with localized current turbulence formed symmetrical, asymmetrical, and interference ripple patterns (Sr; Wilson, 1993). The development of soils (Sp, Ip, lhe) as ponds dried-out obliterated many primary bedding structures.

4 | DEPOSITIONAL MODEL FOR THE GHAGGAR-HAKRA FORMATION

All the field observations support the presence of a fluvial system where the transport and deposition of sediment takes place within erosive channels by the development of in-channel barforms (Ch), accompanied by bedload transport (Gb). The fluvial channels are accompanied by laterally accreting bars (Pb) with chute channels (Cc), channel margin sediments (Cm), and sheet flows (Sf). The elements are arranged to form distinct “channel belt” depositional elements (terminology of Grotzinger et al., 2005; Posmentier & Kolla, 2003). Each belt is separated by “floodplain” depositional elements dominated by fine-grained sediments deposited in bodies of standing water (Po) or by unconfined flooding (Ob). Three channel belt depositional elements are recognized that correspond to the informal lithostratigraphical subdivisions of Bladon, Burley, et al.

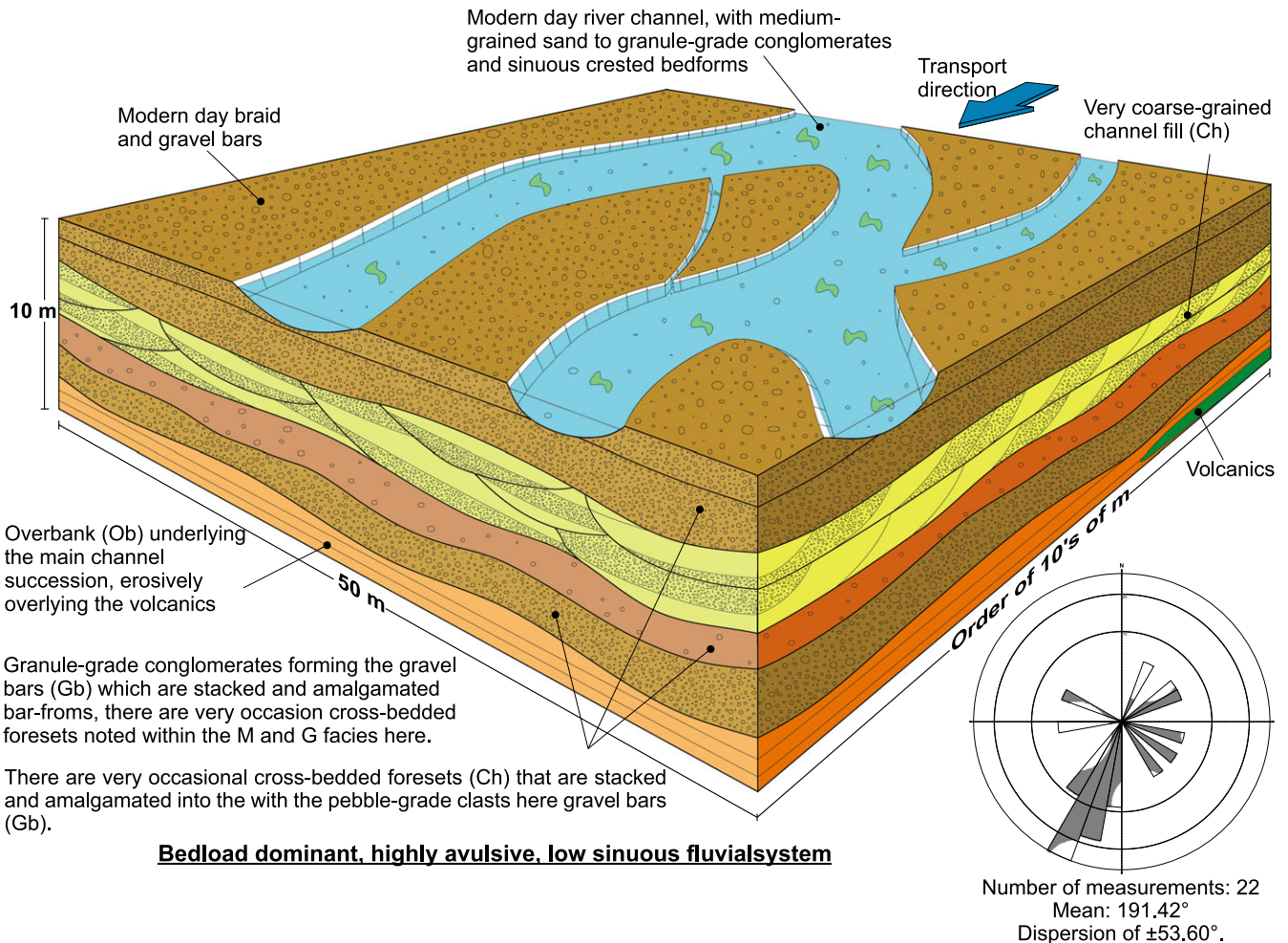


FIGURE 8 Facies model of the gravel bedload dominant low sinuosity fluvial system, the Darjaniyon-ki Dhani Sandstone, which contains the channel (Ch), gravel bar (Gb) and the overbank (Ob) architectural elements. There are 4th to 6th order bounding surfaces within. The sets and cosets within are inconsistent suggesting the gravel bars are transient, suggesting fluvial immaturity. The proportion of channels to floodplain is 90% to 10%, respectively

(2015); Bladon, Clarke, et al. (2015): the Darjaniyon-ki Dhani, Sarnoo and Nosar sandstones. Conceptual facies models for these depositional elements are presented in Figures 8–10 along with a description of the key features and element relationships that define them. An interpretation of each is given below.

The Darjaniyon-ki Dhani Sandstone is dominated by stacked and amalgamated channels and gravel bars indicating a highly mobile, bedload-dominated system where barform migration was transient (Best, Ashworth, Bristow, & Roden, 2003; Bridge, 1993). Transient bars, coupled with a scarcity of completely preserved elements, a range of grain sizes and rare preservation of overbank suggest a highly avulsive system perhaps controlled by frequent changes in energy (Cant & Walker, 1978). The dominance of gravel bar elements (Gb) comprising sediments of debris-driven processes (Tables 1 and 2) indicates a high sediment load (Gulliford, Flint, & Hodgson, 2014; Lowe, 1988; Mather, Stokes, Pirrie, & Hartley, 2008) representing a bedload-dominated, low sinuosity fluvial system (fig. 8 of Miall, 1985).

The sediments of the Sarnoo Sandstone are dominated by stacked and amalgamated transient gravel bars in the

initial deposits indicating a significant degree of channel avulsion. Sinuosity and stability increase up-section to develop channels of stable flow with associated point bars and chute channels (Ielpi & Ghinassi, 2014; fig. 13 of Miall, 1985). However, discharge is still sufficiently irregular to cause sheet flows (Sf) and support ponding on the floodplain; overall this system represents a mixed load, high sinuosity fluvial system (fig. 11 of Miall, 1985).

The Nosar Sandstone displays channels with some degree of stability but separated by transient bars. The system was influenced by avulsion and flooding (Best et al., 2003; Bridge, 1993). Sparse preservation of the overbank may indicate limited and patchy development, or poor preservation because of frequent fluvial avulsion. All features indicate a bedload-dominant, low sinuosity fluvial system (fig. 9 of Miall, 1985).

Channel belt elements are separated by significant sections of floodplain sediments (Figure 2b), that formed through cumulative soil growth and were likely imperfectly to poorly drained due to being seasonally wet. Cyclicity suggests regular flooding which supplied the floodplains with new sediment and recharged ponds, probably a

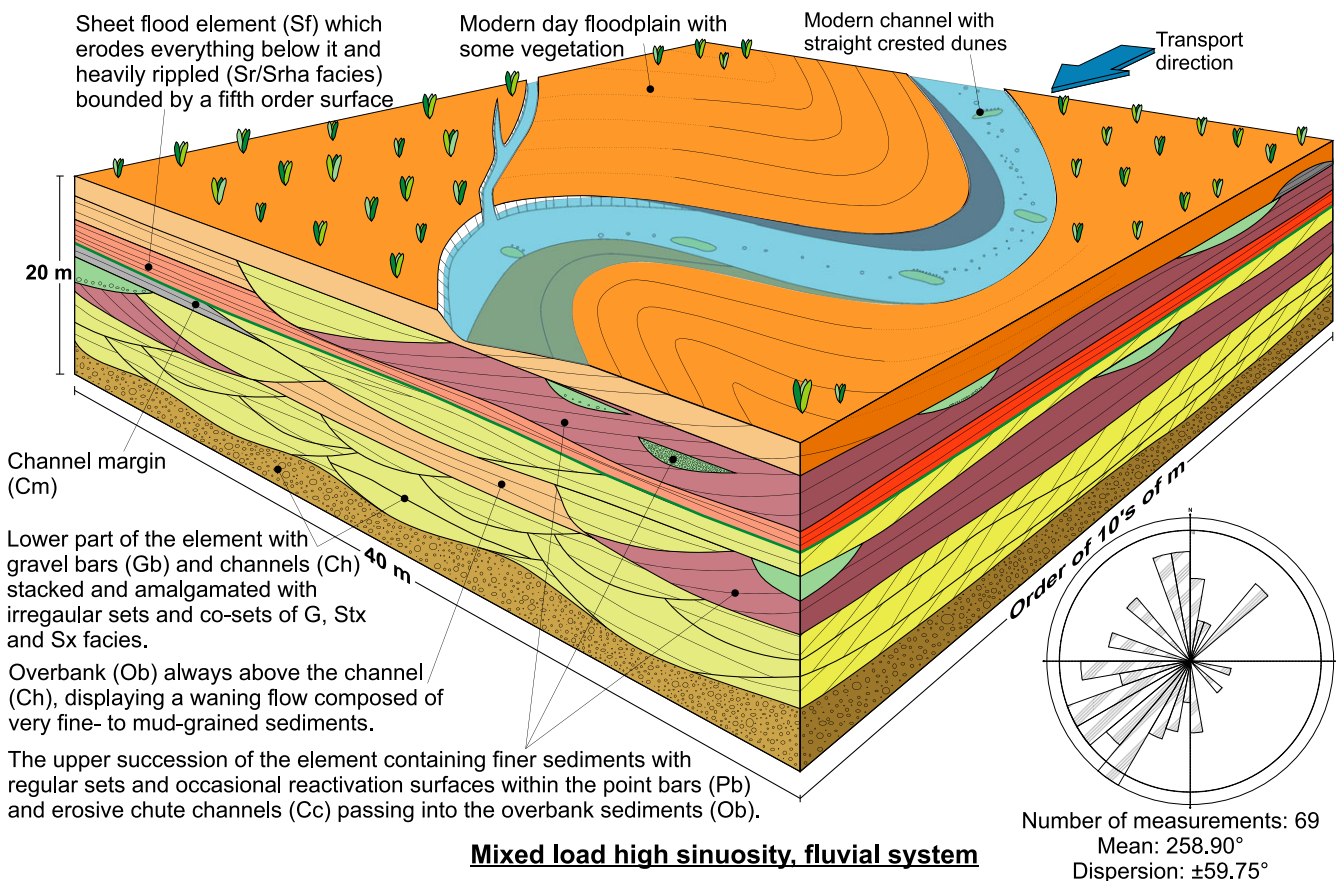


FIGURE 9 Facies model of the mixed load high sinuosity fluvial system, the Sarnoo Sandstone, as evidenced by the channels (Ch), channel margin (Cm), gravel bars (Gb), chute channels (Cc) sheet flows (Sf), and overbank (Ob) elements. The consistency of sets and cosets representing the migration of in-channel bedforms suggests discharge stability. The proportion of sand to mud increases from 80% sand and 20% mud to 60% sand and 40% mud vertically throughout the facies model

consequence of channel instability caused by variations in discharge and sediment load. The thickness of preserved floodplain suggests that the channel belts themselves were reasonably stable for significant periods.

The change in fluvial style from the Darjaniyon-ki Dhani to the Sarnoo sandstones, particularly the increase in sinuosity and the decrease in the dominance of bedload transport, indicates progressive maturing of the Ghaggar-Hakra fluvial system through time (Schumm, 1981). This interpretation is supported by evidence for less flooding and fewer floodplain ponds up-section. However, a decrease in sinuosity from the Sarnoo to Nosar sandstones, coupled with an increase in the proportion of bedload, an increase in bedform and barform migration, and stacking at all scales is atypical of increasing fluvial maturity (Figure 11) and indicates rejuvenation of the whole system.

5 | DISCUSSION

5.1 | The Ghaggar-Hakra succession

The Ghaggar-Hakra Formation records the maturing evolution of an early Cretaceous fluvial system, followed by a

sudden rejuvenation, preserved on an atypical relay ramp on the margin of the Barmer Basin. Dating indicates the succession is of Aptian-Albian age. Deposition of fluvial sediments always represents the complex interplay between the intrinsic processes of sediment transport and deposition and allogenic-controls acting at a variety of spatial and temporal scales (Leeder, 1993). Notwithstanding the constraints of the limited spatial extent of the outcrop available in this study, the relative dominance of broad-scale allocyclic-controls of climate and tectonics (Gawthorpe & Leeder, 2000; Robinson & McCabe, 2012) and the implications for the evolution of the Barmer Basin, warrant some discussion as presented below.

During deposition of the Ghaggar-Hakra Formation, initial rifting between India and Madagascar had started but India and Madagascar remained a single island continent (Biswas, 1987; Bladon, Clarke, et al., 2015). The WIRS was located ~40° south of the equator with the Indo-Tethyan Ocean to the north, and the Aravalli Mountain Range and continental India to the south, in a position between the subtropical arid and temperate climatic belts (Acharyya & Lahiri, 1991; Chatterjee et al., 2013). The abundance of plant remains in the Ghaggar-Hakra Formation indicates that the

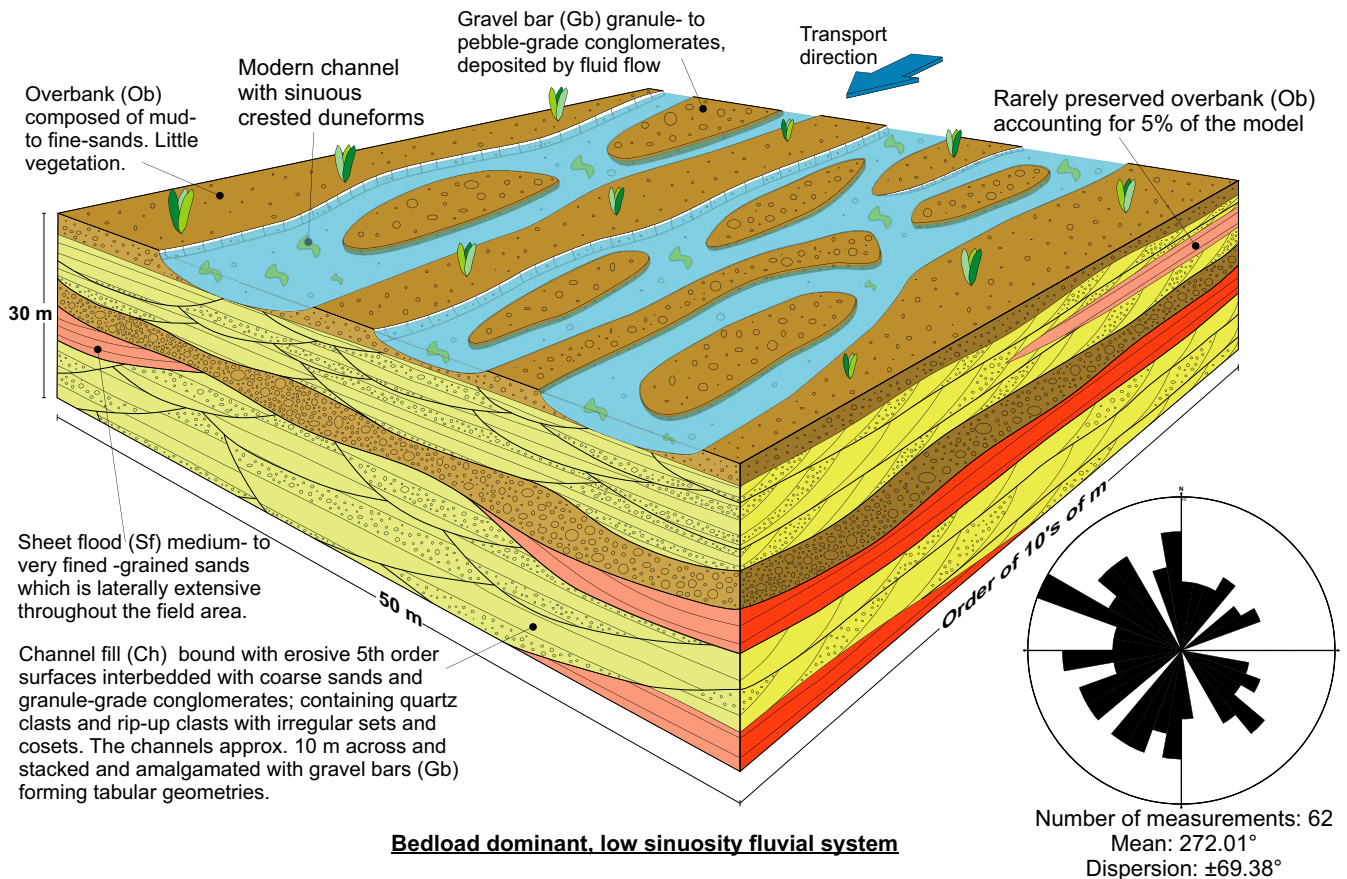


FIGURE 10 Facies model of a well-developed, bedload dominant, low sinuosity fluvial system, the Nosar Sandstone, displays channel (Ch), floodplain (Ob), gravel bars (Gb) and sheetflow (F6) elements. There are all six types of bounding surfaces within indicating erratic surfaces and multiple truncations. This suggests discharge irregularity and a high level of channel migration. The proportion of sand to mud is at 90:10

floodplains were extensive and highly vegetated, with abundant palms and conifers.

Studies and models from other fluvial systems evolving under well-vegetated sub-tropical regimes (Fielding, Allen, Alexander, & Gibling, 2009) display a range of characteristics that are like many of those observed in the Ghaggar-Hakra, including stacked and amalgamated channels with convolute bedding, tree stumps, imperfectly to poorly drained palaeosols (Kraus & Hasiotis, 2006) and variable but significant amounts of floodplain deposition.

However, preserved floodplain thicknesses predicted from fluvial models for subtropical conditions are notably thinner than those observed in the Ghaggar-Hakra (Fielding et al., 2009), and the thick cyclic floodplain successions formed are attributed to periodic flooding, the result of channel instability caused by temporal variations in discharge and sediment load.

Changes in discharge and load may relate to local and/or regional controls of either tectonics or climate. Given that the floodplain is very uniform, with a lack of internal

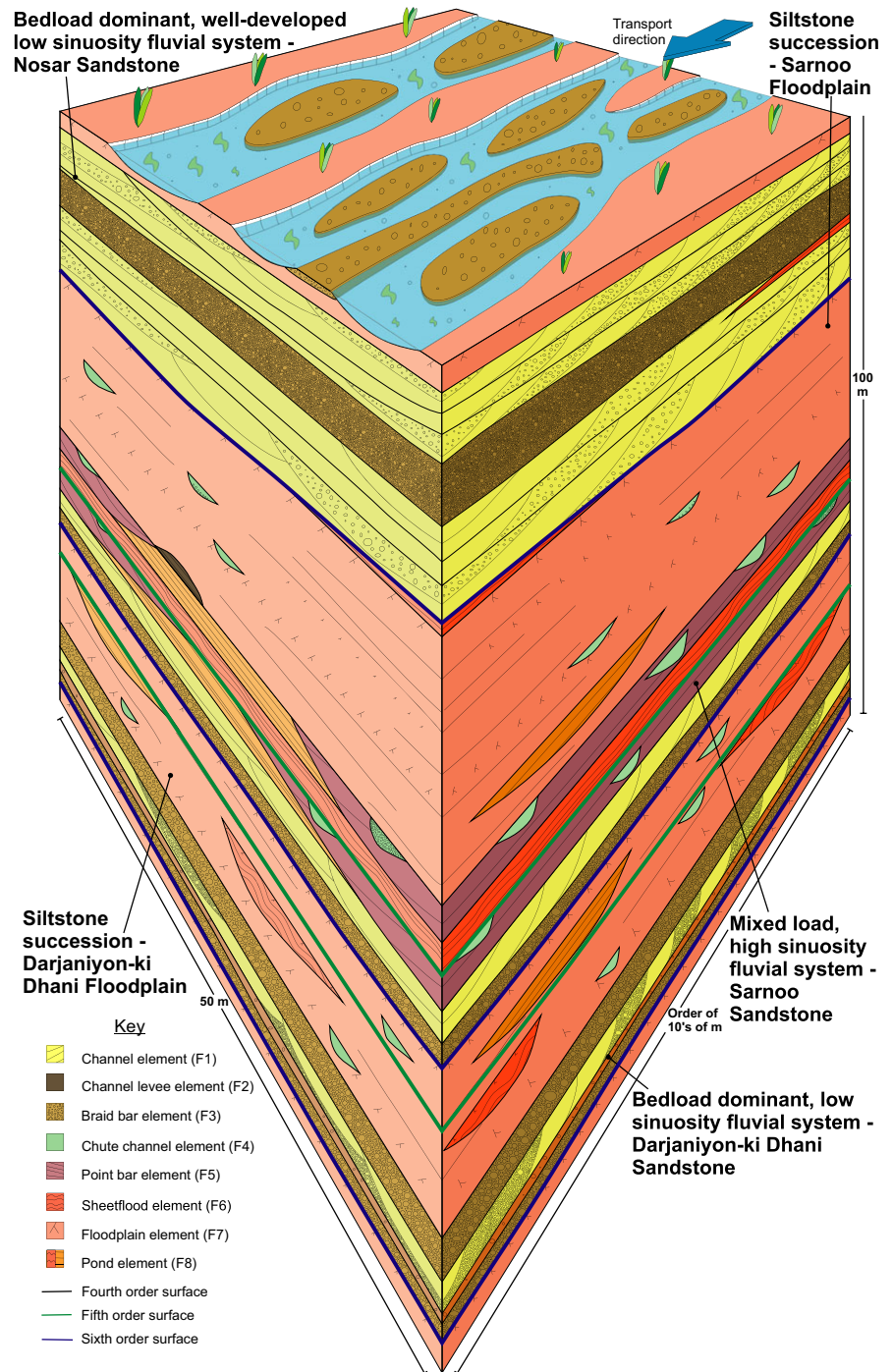


FIGURE 11 Depositional model of the Ghaggar-Hakra Formation displaying the Darjaniyon-ki Dhani and Sarnoo sandstone and their associated floodplain silt packages and the Nosar sandstone capping the formation. The first depositional element is the bedload dominant, low sinuosity fluvial system facies model relating to the Darjaniyon-ki Dhani Sandstone. The third depositional element is the mixed load, high sinuosity fluvial system facies model which directly relates to the Sarnoo Sandstone. The fifth depositional element is formed from the bedload dominant, well-developed, low sinuosity fluvial system relating to the Nosar Sandstone. The intervening siltstones are the floodplain packages: The Darjaniyon-ki Dhani and Sarnoo floodplains. From the Darjaniyon-ki Dhani Sandstone through to the top of the Sarnoo Floodplain a maturation of the fluvial system is recognised. The Nosar Sandstone depositional element represents rejuvenation of the fluvial system

variation in its pedogenic nature, and that the Indian Plate was within the sub-tropical arid and temperate climate belt (Chatterjee et al., 2013; Scotese, 2011; Scotese, Illich, Zumberge, & Brown, 2007) throughout the time of deposition; it is argued that climatic variation is unlikely to have had a significant influence upon the fluvial rejuvenation. However, the climate did influence overbank conditions and soil growth. Based on the palaeosol profile exhibited by overbank elements, the floodplain likely formed oxisols that imply it received at least 100 mm per month of rain over 7 months of the year (Cecil & Dulong, 2013).

In the absence of climate control upon the rejuvenation of the fluvial system during Nosar times, local or regional tectonics is the most likely influence on accommodation space and sedimentation. Recent studies indicate a Mesozoic section is preserved in the subsurface up to 6 km deep, in the centre of the Barmer Basin (Bladon, Clarke, et al., 2015; Kothari et al., 2015) and recognize a west-striking, pre-Palaeogene tectonic grain on the eastern margin (termed the Saraswati Terrace Bladon, Clarke, et al., 2015) that is overprinted by the younger Palaeogene extensional event. Bladon, Burley, et al. (2015) conclude that early northwest–southeast rifting is a consequence of the trans-tensional structural regime that existed between Greater India and Madagascar prior to their separation and the main phase of Deccan volcanic eruption. The sedimentological work on the Ghaggar-Hakra presented herein indicates that this early rift event did indeed influence depositional style and architecture as many of the sedimentary characteristics of the Nosar Sandstone, and rejuvenation of the system, can be explained by deposition on a tectonically subsiding continental alluvial plain.

However, there is no direct evidence from outcrop for stratal growth patterns in the Ghaggar-Hakra, or for a strong relationship between fluvial drainage patterns and fault geometry in the Darjaniyon-ki Dhani to Sarnoo sandstones, which is atypical as these features are generally common in fluvial systems strongly controlled by contemporaneous rifting (Gawthorpe & Leeder, 2000). Apart from the high-energy system recorded in the initial deposits of the Darjaniyon-ki Dhani Sandstone, the succession through to the base of the Nosar Sandstone exhibits progressive fluvial maturation suggesting stability and quiescence. It is only during Nosar times that significant rejuvenation of the fluvial system occurs and that can be attributed to tectonically induced changes in fluvial gradient (Bridge & Leeder, 1979; Leeder, 1993; Schumm, 1993). Consequently, it is tempting to conclude that the base of the Nosar Sandstone, rather than the base of the Ghaggar-Hakra, represents the onset of active rifting in the Barmer Basin during the early northwest–southeast phase of extension recognized by Bladon, Burley, et al. (2015). Alternatively, rift flank uplift accelerated significantly at the base of the Nosar

Sandstone, indicating syn-rift deposition during Lower Cretaceous times. This in turn implies high preservation potential for thick early Cretaceous fluvial successions within rifted fault blocks beneath the Palaeogene fill that likely have significant potential for further hydrocarbon exploration.

5.2 | Implications for Palaeogeography of the north-west Indian Plate in the Lower Cretaceous Epoch

During Early Cretaceous times, clastic deposition across the north-west Indian Plate was dominated by fluvial systems carrying sediment to coastal plains and deltas forming along the edge of the Indo-Tethyan Ocean. In the Kachchh and the Middle and Lower Indus basins, the Lower Cretaceous Bhuj and Lower Goru formations are established reservoirs for hydrocarbons (Ahmad et al., 2012; Biswas, 1999; Mukherjee, 1983). However, Cretaceous sediments are rarely exposed at outcrop across the Indian Plate, being preserved only within rift basins or at basin margins, where they have been downfaulted and protected from the effects of Palaeogene and Neogene uplift and erosion. Therefore, reconstructing even local Cretaceous palaeogeography is difficult because of limited outcrop, and collation of descriptions of the Lower Cretaceous sediments is required.

In addition to the Ghaggar-Hakra, Lower Cretaceous fluvial deposits are present in the Kachchh (Aslam, 1992; Casshyap & Aslam, 1992) Cambay (Bhatt et al., 2016; Jana, King, & Hilton, 2013; Mukherjee, 1983) and Narmada (Akhtar & Ahmad, 1991; Racey, Fisher, Bailey, & Kumar-Roy, 2016) basins and shallow marine sedimentation occurred within the Kachchh (Racey et al., 2016; Rai, 2006), Jaisalmer (Singh, 2006), and Indus (Ahmad, Fink, Sturrock, Mahmood, & Ibrahim, 2004; Ahmad et al., 2012) basins. There is also evidence for ~1 km of Mesozoic sediments beneath the main Deccan volcanic pile as indicated by geophysical mapping (Rajaram, Anand, Erram, & Shinde, 2016; Rao, Kumar, & Rastogi, 2015). Therefore, it is pertinent to ask the following question, initially posed by Biswas (1999): was the Ghaggar-Hakra Formation only deposited in the rift systems or was it widespread across the north-west Indian Plate?

The depth to top basement map for north-west India of Kothari et al. (2015) is used to establish a detailed structural framework to depict the early Cretaceous rift systems which in turn define the depositional systems and their distribution (Figure 12). The extent, type, and distribution of the depositional systems are initially established from the Sarnoo Hills work, together with published accounts of early Cretaceous outcrop and subsurface sediments, before speculatively extrapolating facies following Walther's Law.

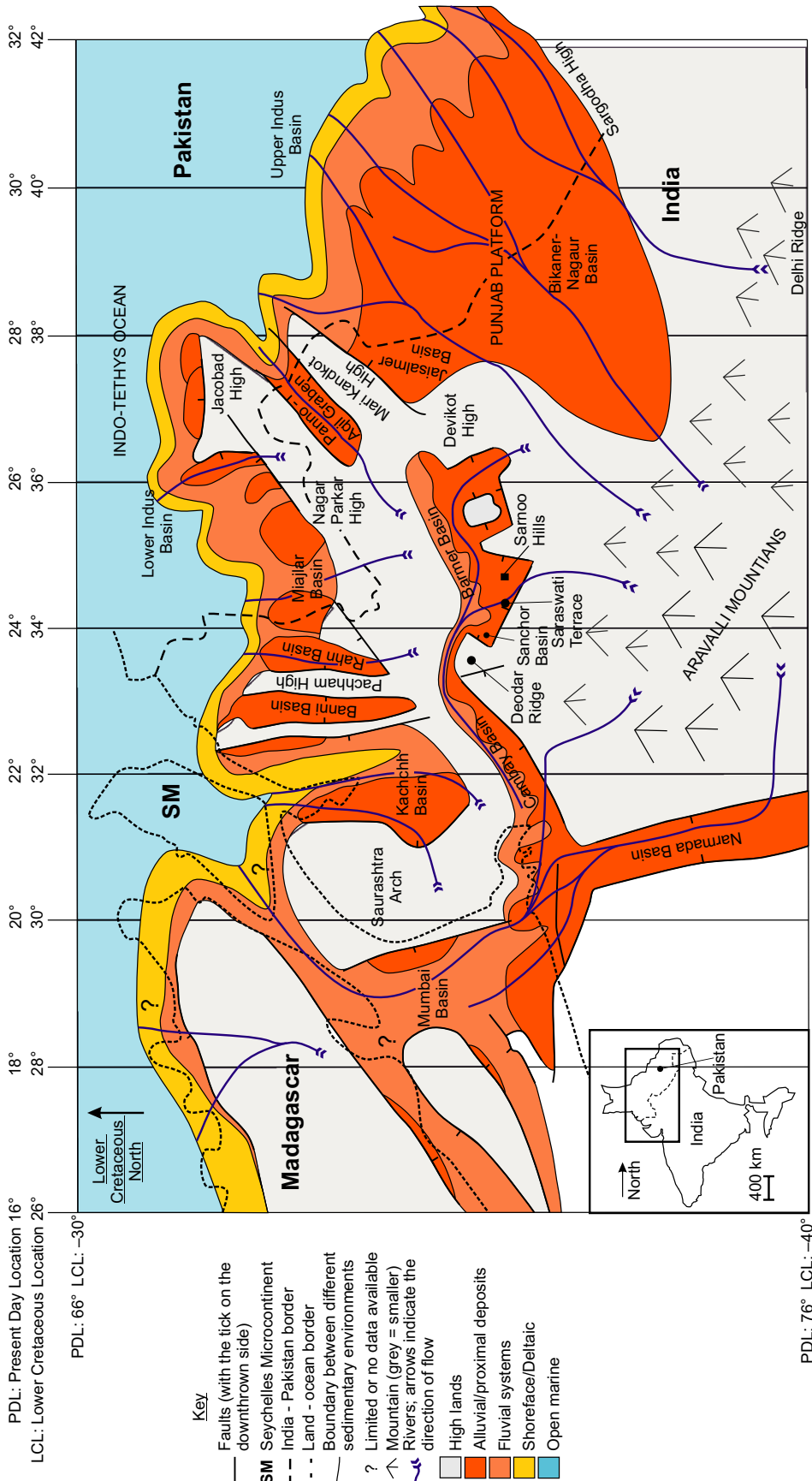


FIGURE 12 Palaeogeographical reconstruction of the Lower Cretaceous rift and depositional systems, in the north-western Indian Plate. Distribution of the dominant facies, i.e. alluvial passing into fluvial sedimentation, is based on Walther's Law constrained by the disparate outcrops. The Indo-Tethys Ocean coastline is depicted by coastal sedimentation within the Indus, Jaisalmer, Miajliar, Rahn, Banni and Kachchh basins; these coastal sediments pass into shallow and deep sediments in present day Pakistan. The rivers feeding these basins and coastal sediments are sourced from the Aravalli Mountain Range with palaeocurrents ranging from southwest to northwest. This palaeogeographical reconstruction of the sediments is derived from Ahmad et al. (2012); Akhtar & Ahmed (1991); Aslam (1992); Bhatt et al. (2016); Biswas (1999); Casshyap & Aslam (1992); Chatterjee et al. (2013); Khalid et al. (2014); Kothari et al. (2015); Mukherjee (1983); Racey et al. (2016); Rai et al. (2013); Rajaram et al. (2017); Rao et al. (2015)

During Cretaceous times, the Indian Plate was rotated 90° clockwise with respect to its present orientation (Figure 12; Chatterjee et al., 2013), so its leading edge comprised much of present-day Pakistan where the Lower Cretaceous sediments were deposited in coastal embayments, deltas, and shorefaces (Ahmad et al., 2012; Smewing, Warburton, Daley, Copestake, & Ul-haq, 2002). As India was within the subtropical arid and temperate climate belt, the overall precipitation across India was low to medium (1.5–12 cm/month; Chatterjee et al., 2013). The FOAM palaeoclimate simulations (Goswami, 2011; Scotese, 2011; Scotese et al., 2007) indicate that the WIRS and surrounding areas were comparatively dry and warm (17°C) when compared to the east of the India which is separated from them by the 600 km long Aravalli Mountain Range.

Along the northern leading edge of the Indian Plate, the coastal Sembar Formation siliciclastics were deposited on top of an extensive carbonate platform (Khalid et al., 2014). This resulted from a gradual and long-term base-level rise leading to high-stand shedding with the formation of a westerly prograding delta (the “Goru Fan Delta”). An active longshore drift and tidal influence restricted these sands to the east of the shelf where they formed a ramp ~200 km wide (Ahmad et al., 2004) that gradually deepened to the west and north (fig. 9 of Khalid et al., 2014). The Goru Fan Delta fed by fluvial systems draining the north-west Indian Plate built out into the marine embayment, across the Jaisalmer Basin and the Punjab Platform and is imaged on regional two-dimensional seismic data (Figure 12; Khalid et al., 2014). Consequently, the Lower Cretaceous shoreline, shelf edge positions, and lateral shifts are reasonably well-known across the north-west Indian Plate in south-central Pakistan (Khalid et al., 2014). Fluvial palaeocurrent directions across the Lower Goru Fan Delta are from the east and south-east consistent with sources on the Indian Plate (Ahmad et al., 2004). The Ghaggar-Hakra Formation palaeocurrent directions, present day, are to the south-west (Figures 7–9; Bladon, Burley, et al., 2015; Sisdia & Singh, 2000) into the Barmer Basin reflecting their location on a feeder relay ramp (Saraswati Terrace) into the rift and directed towards the Cambay Basin. Therefore, it is possible to speculate that these sediments actually fed the southerly part of the WIRS and potentially drained into a poorly known early Cretaceous rift basin beneath the present-day Gulf of Khambhat. Early Cretaceous rivers draining the Devikot High and the northern Aravalli Range likely supplied the Lower Goru and Sembar formations across the Punjab Platform (Figure 12).

This palaeogeographical reconstruction suggests a much more complex drainage system than has previously been envisaged for the northern leading edge of the Indian Plate. Upland deposits had a very low preservation potential

which, compounded with later uplift and widespread erosion preceding the Deccan volcanism, resulted in the disparate preservation of fluvial early Cretaceous sediments. Along with Biswas (1999), it is proposed here that most of the early Cretaceous sediments preserved in the WIRS are indeed remnants of a syn-rift continental succession. By contrast, the coastal plain and deltaic deposits of the Sembar-Lower Goru succession were much more regionally extensive at deposition and accumulated along the Indo-Tethyan leading edge in coastal plain, deltaic, and shallow marine shoreface settings.

6 | CONCLUSIONS

The outcrops at Sarnoo, Karentia, and Nosar provide continuous sections and significant insight through Lower Cretaceous fluvial strata of the Ghaggar-Hakra Formation. The sedimentary succession includes channels, bars, sheet floods, and overbank deposits in varied proportions that typify a fluvial system deposited under sub-tropical climate conditions. The immature, low sinuosity system of the Darjaniyon-ki Dhani Sandstone, dominated by gravel bars and isolated channels, along with its frequently flooded and poorly drained floodplain, matures upward into the laterally migrating channel system of the highly sinuous Sarnoo Sandstone. The Nosar Sandstone completes the formation at outcrop and comprises stacked and amalgamated channels and gravel bars indicating fluvial rejuvenation.

Fluvial rejuvenation is most likely a response to faulting and it is concluded tentatively that the Nosar Sandstone may represent the onset or acceleration of rifting and development of the eastern margin of the Barmer Basin. Consequently, the Nosar Sandstone, along with contemporaneous and later sediments of the Ghaggar-Hakra Formation, is syn-rift in nature. This conclusion supports that of Bladon, Burley, et al. (2015) derived from structural analysis and provides further evidence that extension in the Barmer area of north-west India was probably established prior to the start of the Palaeogene Period. Given this interpretation, well-developed successions of Cretaceous fluvial strata may be preserved in Mesozoic sections of the subsurface of the WIRS, offering hydrocarbon potential below the presently explored Palaeogene succession of the Barmer and related basins.

Early Cretaceous sediments are rarely exposed at outcrop across the north-west Indian Plate. Comparisons between the Ghaggar-Hakra Formation and other successions of comparable age, between their relative positions in a plate tectonic framework, and with regional structural data, allow for a reconstruction of a detailed palaeogeographical map for this part of the north-west Indian Plate for the early Cretaceous. The reconstruction suggests

a more complex fluvial drainage system than previously envisaged, with continental early Cretaceous sediments preserved only within contemporaneous rifts.

ACKNOWLEDGEMENTS

This research was undertaken with matched funding from the Keele University Acorn Fund and Cairn India Limited. Cairn India Limited also generously provided logistical support for all fieldwork in Rajasthan for which the authors are very grateful. Bhanwar Lal, Andrew Bladon, and James Solan are thanked for their practical assistance and good humour in the field. Colleagues within the Basin Dynamics Research Group at Keele and RPS Ichron are also thanked for helpful discussions on sedimentology and basin analysis as our thoughts on the Cretaceous of the Barmer Basin evolved. We extend our appreciation to the two referees and journal editor Peter Swart for their valuable comments on the original manuscript.

CONFLICT OF INTEREST

We (the authors) have no conflict of interest to declare.

REFERENCES

- Acharyya, S. K., & Lahiri, T. C. (1991). Cretaceous palaeogeography of the Indian subcontinent: A review. *Cretaceous Research*, *12*, 3–26. [https://doi.org/10.1016/0195-6671\(91\)90024-7](https://doi.org/10.1016/0195-6671(91)90024-7)
- Ahmad, A. H. M. (1988). *Facies analysis, sedimentation and diagenesis of Cretaceous sandstones of north-eastern Gujarat*. PhD thesis, Aligarh Muslim University.
- Ahmad, R., & Amad, J. (1991). Petroleum geology and prospects of the Sukkur Rift Zone, Pakistan, with special reference to the Jaisalmer, Cambay and Bombay High basins of India. *Pakistan Journal of Hydrocarbon Research*, *3*(2), 33–41.
- Ahmad, N., Fink, P., Sturrock, S., Mahmood, T., & Ibrahim, M. (2004). Sequence stratigraphy as predictive tool in Lower Goru Fairway, Lower and Middle Indus Platform, Pakistan. Annual Technical Conference, ATC, 2004. 8–9 October, Islamabad.
- Ahmad, N., Fink, P., Sturrock, S., Mahmood, T., & Ibrahim, M. (2012). Sequence stratigraphy as predictive tool in Lower Goru Fairway, Lower and Middle Indus Platform, Pakistan. AAPG Search and Discovery Article #10404.
- Ahmad, N., & Khan, M. R. (2012). Evaluation of a distinct sub-play for enhanced exploration in an emerging petroleum province, Bannu-Kohat sub-basin, Pakistan. American Association of Petroleum Geology, Search and Discovery Article 10391, conference paper.
- Akhtar, K., & Ahmad, A. H. M. (1991). Single-cycle cratonic quartzarenites produced by tropic weathering: The Nimar sandstones (Lower Cretaceous), Narmada Basin, India. *Sedimentary Geology*, *71*, 23–32. [https://doi.org/10.1016/0037-0738\(91\)90004-W](https://doi.org/10.1016/0037-0738(91)90004-W)
- Ali, J. R., & Aitchison, J. C. (2014). Greater India's northern margin prior to its collision with Asia. *Basin Research*, *26*, 73–84. <https://doi.org/10.1111/bre.12040>
- Aslam, M. (1992). Delta plain coal deposits from the than formation of the Early Cretaceous Saurashtra Basin, Gujarat, western India. *Sedimentary Geology*, *81*, 181–193. [https://doi.org/10.1016/0037-0738\(92\)90069-4](https://doi.org/10.1016/0037-0738(92)90069-4)
- Baksi, S. K., & Naskar, P. (1981). Fossil plants from the Sarnu Hill formation, Barmer Basin, Rajasthan. *The Palaeobotanist*, *27*, 107–111.
- Balakrishnan, T. S., Unnikrishnan, P., & Murty, A. V. S. (2009). The tectonic map of India and contiguous areas. *Journal of the Geological Society of India*, *74*, 158–170. <https://doi.org/10.1007/s12594-009-0119-4>
- Banham, S. G., & Mountney, N. P. (2013). Climatic versus halokinetic control on sedimentation in a dryland fluvial succession: Triassic Moenkopi Formation, Utah, USA. *Sedimentology*, *61*, 570–608.
- Bastia, R., Reeves, C., Pundarika, R. D., D'Silva, K., & Radhakrishna, M. (2010). Paleogeographic reconstruction of east Gondwana and evolution of the Indian Continental margin. DCS-DST News, 2–8.
- Basu, A. R., Renne, P. R., DasGupta, D. K., Teichman, F., & Poreda, R. J. (1993). Early and late alkali igneous pulses and a high ³He plume origin for the Deccan Flood basalts. *Science*, *261*, 902–906. <https://doi.org/10.1126/science.261.5123.902>
- Best, J. L., Ashworth, P. J., Bristow, C. S., & Roden, J. (2003). Three-dimensional sedimentary architecture of a large, mid-channel sand braid bar, Jamuna River, Bangladesh. *Journal of Sedimentary Research*, *73*, 516–530. <https://doi.org/10.1306/010603730516>
- Bhatt, N. Y., Solanki, P. M., Prakash, N., & Das, N. (2016). Depositional environment of Himmantnagar Sandstone (Lower/Middle Cretaceous): A perspective. *The Palaeobotanist*, *56*, 67–84.
- Biswas, S. K. (1982). Rift basins in Western Margin of India and their hydrocarbon prospects with special reference to Kutch Basin. *American Association of Petroleum Geology Bulletin*, *66*, 1497–1513.
- Biswas, S. K. (1987). Regional tectonic framework, structure and evolution of the western marginal basins of India. *Tectonophysics*, *135*, 307–327. [https://doi.org/10.1016/0040-1951\(87\)90115-6](https://doi.org/10.1016/0040-1951(87)90115-6)
- Biswas, S. K. (1999). A review on the evolution of rift basins in India during Gondwana with special reference to the western Indian basins and the hydrocarbon prospects. *PINAS*, *3*, 261–283.
- Bladon, A. J., Burley, S. D., Clarke, S. M., & Beaumont, H. (2015). Geology and regional significance of the Sarnoo Hills, eastern rift margin of the Barmer Basin, northwest India. *Basin Research*, *27*, 636–655. <https://doi.org/10.1111/bre.12093>
- Bladon, A. J., Clarke, S. M., & Burley, S. D. (2015). Complex rift geometries resulting from inheritance of pre-existing structures: Insights and regional implications from the Barmer Basin rift. *Journal of Structural Geology*, *71*, 136–154.
- Blair, T. C. (2000). Sedimentary and progressive tectonic unconformities of the sheet flood-dominated Hell's Gate alluvial fan, Death Valley, California. *Sedimentary Geology*, *132*, 233–262. [https://doi.org/10.1016/S0037-0738\(00\)00010-5](https://doi.org/10.1016/S0037-0738(00)00010-5)
- Blair, T. C., & McPherson, J. G. (1994). Alluvial fans and their natural distinctions from rivers based on morphology, hydraulic processes, sediment processes and facies assemblages. *Journal of Sedimentary Research*, *A64*, 450–489.
- Bordy, E. M., Hancox, P. J., & Rubidge, B. S. (2004). Fluvial style variations in the Late Triassic-Early Jurassic Elliot Formations, main Karoo Basin, South Africa. *Journal of African Earth*

- Sciences*, 38, 383–400. <https://doi.org/10.1016/j.jafrearsci.2004.02.004>
- Bridge, J. S. (1993). The interaction between channel geometry, water flow, sediment transport and deposition in braided rivers. *Geological Society London, Special Publication*, 75, 13–71. <https://doi.org/10.1144/GSL.SP.1993.075.01.02>
- Bridge, J. S., Alexander, J., Collier, R. E. L. L., Gawthorpe, R. L., & Jarvis, J. (1995). Ground-penetrating radar and coring used to study the large-scale structure of point-bar deposits in three dimensions. *Sedimentology*, 42, 839–852. <https://doi.org/10.1111/j.1365-3091.1995.tb00413.x>
- Bridge, J. S., & Best, J. L. (1988). Flow, sediment transport and bedform dynamics over the transition from dunes to upper-stage plane beds: Implications for the formation of planar laminae. *Sedimentology*, 35, 753–763. <https://doi.org/10.1111/j.1365-3091.1988.tb01249.x>
- Bridge, J. S., & Leeder, M. R. (1979). A simulation of model alluvial stratigraphy. *Sedimentology*, 26, 617–644. <https://doi.org/10.1111/j.1365-3091.1979.tb00935.x>
- Brierley, G., Fergusin, R. J., & Woolfe, K. J. (1997). What is a fluvial levee? *Sedimentary Geology*, 114, 1–9. [https://doi.org/10.1016/S0037-0738\(97\)00114-0](https://doi.org/10.1016/S0037-0738(97)00114-0)
- Bromley, R. G., & Asgaard, U. (1979). Triassic freshwater ichno-coenoses from Carlsberg Fjord, East Greenland. *Palaeogeography, Palaeoclimate, Palaeoecology*, 28, 39–80. [https://doi.org/10.1016/0031-0182\(79\)90112-3](https://doi.org/10.1016/0031-0182(79)90112-3)
- Bromley, R. G., & Asgaard, U. (1991). Ichnofacies: A mixture of taphofacies and biofacies. *Lethaia*, 24, 153–163. <https://doi.org/10.1111/j.1502-3931.1991.tb01463.x>
- Buatois, L. A., & Mangano, M. G. (2002). Trace fossils from Carboniferous floodplain deposits in Western Argentina: Implications for ichnofacies models of continental environments. *Palaeogeography, Palaeoclimate and Palaeoecology*, 183, 71–86. [https://doi.org/10.1016/S0031-0182\(01\)00459-X](https://doi.org/10.1016/S0031-0182(01)00459-X)
- Cant, D. J., & Walker, R. G. (1978). Fluvial processes and facies sequences in the sandy South Saskatchewan River, Canada. *Sedimentology*, 25, 625–648. <https://doi.org/10.1111/j.1365-3091.1978.tb00323.x>
- Casshyap, S. M., & Aslam, M. (1992). Deltaic and shoreline sedimentation in Saurashtra Basin, western India: An example of infilling in an early Cretaceous failed rift. *Journal of Sedimentary Petrology*, 62, 972–991. <https://doi.org/10.1306/D4267A2D-2B26-11D7-8648000102C1865D>
- Cecil, C. B., & Dulong, F. T. (2013). Precipitation models for sediment supply in warm climates. *Climate Controls on Stratigraphy*, SEPM Special Publication No. 77, 21–27.
- Chatterjee, S., Goswami, A., & Scotese, C. R. (2013). The longest voyage: Tectonic, magmatic, and paleoclimatic evolution of the Indian plate during its northward flight from Gondwana to Asia. *Gondwana Research*, 23, 238–267. <https://doi.org/10.1016/j.gr.2012.07.001>
- Chowdhary, L. R. (1975). Reversal of basement-block motions in Cambay Basin, India, and its importance in petroleum exploration. *American Association of Petroleum Geologists Bulletin*, 59, 85–96.
- Collier, J. S., Sansom, V., Ishizuka, O., Taylor, R. N., Minshull, T. A., & Whitmarsh, R. B. (2008). Age of Seychelles-India breakup. *Earth and Planetary Science Letters*, 272, 264–277. <https://doi.org/10.1016/j.epsl.2008.04.045>
- Compton, P. M. (2009). The geology of the Barmer Basin, Rajasthan, India and the origins of its major oil reservoir, the Fatehgarh Formation. *Petroleum Geoscience*, 15, 117–130. <https://doi.org/10.1144/1354-079309-827>
- Crawford, A. R., & Compton, W. (1969). The age of the Vindhyan System of Peninsular India. *Quarterly Journal of the Geological Society*, 125, 351–371. <https://doi.org/10.1144/gsjgs.125.1.0351>
- Dasgupta, S., & Mukherjee, S. (2017). Brittle shear tectonics in a narrow continental rift: Asymmetric non-volcanic Barmer Basin (Rajasthan, India). *The Journal of Geology*, 125, 561–591. <https://doi.org/10.1086/693095>
- Desai, A. G., & Desai, S. J. (1989). *Himatnagar Sandstones of north Gujarat their depositional environment and tectonic framework*. PhD thesis, Maharaja Sayajirao University of Baroda.
- Dev, S. (1987). Floristic zones in the Mesozoic formations and their relative age. *Palaeobotanist*, 36, 161–167.
- Dolson, J., Burley, S. D., Sunder, V. R., Kothari, V., Naidu, B., Whiteley, N. P., ... Ananthakrishnan, B. (2015). The discovery of the Barmer Basin, Rajasthan, India and its petroleum geology. *American Association of Petroleum Geology Bulletin*, 99, 433–465. <https://doi.org/10.1306/10021414045>
- Eagles, G., & Hoang, H. H. (2014). Cretaceous to present kinematics of the Indian, African and Seychelles plates. *Geophysical Journal International*, 196, 1–14. <https://doi.org/10.1093/gji/ggt372>
- Fielding, C. R., Allen, J. P., Alexander, J., & Gibling, M. R. (2009). Facies model for fluvial systems in the seasonal tropics and subtropics. *Geological Society of America*, 37, 623–626.
- Froude, M. J., Alexander, J., Barclay, J., & Cole, P. (2017). Interpreting flash flood palaeoflow parameters from anti-dunes and gravel lenses: An example from Montserrat, West Indies. *Sedimentology*, 64, 1817–1845. <https://doi.org/10.1111/sed.12375>
- Ganerød, M., Torsvik, T. H., van Hinsbergen, D. J. J., Gaina, C., Corfu, F., Werner, S., ... Hendriks, B. W. H. (2011). Palaeoposition of the Seychelles microcontinent in relation to the Deccan Traps and the plume generation zone in the late Cretaceous-early Palaeogene time. *Geological Society of London, Special Publications*, 357, 229–252. <https://doi.org/10.1144/SP357.12>
- Gawthorpe, R. L., & Leeder, M. R. (2000). Tectono-sedimentary evolution of active extensional basins. *Basin Research*, 12, 195–218. <https://doi.org/10.1046/j.1365-2117.2000.00121.x>
- Ghazi, S., & Mountney, N. P. (2009). Facies and architectural element analysis of a meandering fluvial succession: The Permian Warchha Sandstone, Salt Range, Pakistan. *Sedimentary Geology*, 221, 99–126. <https://doi.org/10.1016/j.sedgeo.2009.08.002>
- Ghinassi, M. (2010). Chute channels in the Holocene high-sinuosity river deposits of the Firenze plain, Tuscany, Italy. *Sedimentology*, 58, 618–642.
- Goswami, A. (2011). *Predicting the geographic distribution of ancient soils with special reference to the Cretaceous*. PhD thesis, University of Texas, Arlington, TX.
- Gowland, S., Taylor, A. M., & Martinus, A. W. (2018). Integrated sedimentology and ichnology of Late Jurassic fluvial point-bars – Facies architecture and colonization styles (Lourinha Formation, Lusitanian Basin, western Portugal). *Sedimentology*, 65, 400–430. <https://doi.org/10.1111/sed.12385>
- Grotzinger, J. P., Arvidson, R. E., Bell, J. F. III, Calvin, W., Clark, B. C., Fike, D. A., ... Watters, W. A. (2005). Stratigraphy and sedimentology of a dry and wet eolian depositional system, Burns Formation, Meridiani Planum, Mars. *Earth and Planetary Science Letters*, 240, 11–72. <https://doi.org/10.1016/j.epsl.2005.09.039>

- Gulliford, A. R., Flint, S. S., & Hodgson, D. M. (2014). Testing applicability of models of distributive fluvial systems or trunk rivers in ephemeral systems: Reconstructing 3-D fluvial architecture in the Beaufort Group, South Africa. *Journal of Sedimentary Research*, *84*, 1147–1169. <https://doi.org/10.2110/jsr.2014.88>
- Hallam, A. (1985). A review of Mesozoic climates. *Journal of Geological Society of London*, *142*, 433–445. <https://doi.org/10.1144/gsjgs.142.3.0433>
- Hampton, B. A., & Horton, B. K. (2007). Sheetflood fluvial processes in a rapidly subsiding basin, Altiplano plateau, Bolivia. *Sedimentology*, *54*, 1121–1147. <https://doi.org/10.1111/j.1365-3091.2007.00875.x>
- Hjellbakk, A. (1997). Facies and fluvial architecture of a high-energy braided river: The upper Proterozoic Segloddan Member, Varanger Peninsula, northern Norway. *Sedimentary Geology*, *114*, 131–161. [https://doi.org/10.1016/S0037-0738\(97\)00075-4](https://doi.org/10.1016/S0037-0738(97)00075-4)
- Hunter, R. E. (1977a). Terminology of cross-stratified sedimentary layers and climbing-ripple structures. *Journal of Sedimentary Petrology*, *47*, 697–706.
- Hunter, R. E. (1977b). Basic types of stratification in small eolian dunes. *Sedimentology*, *24*, 361–387. <https://doi.org/10.1111/j.1365-3091.1977.tb00128.x>
- Ielpi, A., & Ghinassi, M. (2014). Planform architecture, stratigraphic signature and morphodynamics of an exhumed Jurassic meander plain (Scalby Formation, Yorkshire, UK). *Sedimentology*, *61*, 1923–1960. <https://doi.org/10.1111/sed.12122>
- Jackson, R. G. (1976). Depositional model of point bars in the lower Wabash River. *Journal of Sedimentary Petrology*, *46*, 579–594.
- Jaitly, A. K., & Ajane, R. (2013). Comments on Placenticerias Mintoi (Vredenburg, 1906) from the Bagh Beds (Late Cretaceous), Central India with special reference to Turonian nodular limestone horizon. *Journal of the Geological Society of India*, *81*, 565–574. <https://doi.org/10.1007/s12594-013-0072-0>
- Jana, B. N., King, S. C., & Hilton, J. (2013). Revision of the Cretaceous fossil plant-assembly from Gardeshwar (Gujarat, India): A conifer dominated floral associations from an Upper Gondwana sequence on the West Coast of India. *Journal of Asian Earth Sciences*, *73*, 128–138. <https://doi.org/10.1016/j.jseaes.2013.04.021>
- Jones, B. G., & Rust, B. R. (1982). Massive sandstone facies in the Hawkesbury Sandstone: A Triassic fluvial deposit near Sydney, Australia. *Journal of Sedimentary Petrology*, *54*(4), 1249–1259.
- Khalid, P., Qayyum, F., & Yasin, Q. (2014). Data-driven sequence stratigraphy of the Cretaceous depositional system, Punjab Platform, Pakistan. *Survey Geophysics*, *35*, 1065–1088. <https://doi.org/10.1007/s10712-014-9289-8>
- Khosla, A., Kapur, V. V., Sereno, P. C., Wilson, J. A., Wilson, G. P., Dutheil, D., ... Rana, R. S. (2003). First dinosaur remains from the Cenomanian Turonian Nimar sandstone (Bagh Beds), District Dhar, Madhya Pradesh, India. *Journal of the Palaeontological Society of India*, *48*, 115–127.
- Kothari, V., Naidu, B., Sunder, V. R., Dolson, J., Surley, S. D., Whiteley, N. P., ... Ananthakrishnan, B. (2015). Discovery and petroleum system of Barmer Basin, India. (abs.). American Association of Petroleum Geology, Search and discovery article #110202, Conference Paper.
- Kraus, M. J. (1999). Paleosols in clastic sedimentary rocks: Their geologic applications. *Earth Science Reviews*, *47*, 41–70. [https://doi.org/10.1016/S0012-8252\(99\)00026-4](https://doi.org/10.1016/S0012-8252(99)00026-4)
- Kraus, M. J., & Aslan, A. (1999). Palaeosol sequences in floodplain environments: A hierarchical approach. *Special Publications International Association of Sedimentologists*, *27*, 303–321.
- Kraus, M. J., & Hasiotis, S. T. (2006). Significance of different modes of rhizolith preservation to interpreting paleoenvironmental and paleohydrologic settings: Examples from Paleogene palaeosols, Bighorn Basin, Wyoming, USA. *Journal of Sedimentary Research*, *76*, 633–646. <https://doi.org/10.2110/jsr.2006.052>
- Leeder, M. R. (1993). Tectonic controls upon drainage basin development, river channel migration and alluvial architecture: Implications for hydrocarbon reservoir development and characterization. *Geological Society, London, Special Publications*, *73*, 7–22. <https://doi.org/10.1144/GSL.SP.1993.073.01.02>
- Lowe, D. R. (1988). Suspended-load fallout rate as an independent variable in the analysis of current structures. *Sedimentology*, *35*, 765–776. <https://doi.org/10.1111/j.1365-3091.1988.tb01250.x>
- Martin, C. A. L., & Turner, B. R. (1998). Origins of massive-type sandstones in braided river systems. *Earth-Science Reviews*, *44*, 15–38. [https://doi.org/10.1016/S0012-8252\(98\)00019-1](https://doi.org/10.1016/S0012-8252(98)00019-1)
- Mather, A., Stokes, M., Pirrie, D., & Hartley, R. (2008). Generation, transport and preservation of armoured mudballs in an ephemeral gully system. *Geomorphology*, *100*, 104–119. <https://doi.org/10.1016/j.geomorph.2007.10.030>
- Miall, A. D. (1985). Architectural-element analysis: A new method of facies analysis applied to fluvial deposits. *Earth Science Review*, *22*, 261–308. [https://doi.org/10.1016/0012-8252\(85\)90001-7](https://doi.org/10.1016/0012-8252(85)90001-7)
- Miall, A. D. (1988). Architectural elements and bounding surfaces in fluvial deposits: Anatomy of the Kayenta Formation (Lower Jurassic), southwest Colorado. *Sedimentary Geology*, *55*, 233–262. [https://doi.org/10.1016/0037-0738\(88\)90133-9](https://doi.org/10.1016/0037-0738(88)90133-9)
- Mishra, P. C., Singh, N. P., Sharma, D. C., Kakaroo, A. K., Upadhyay, H., & Saini, M. L. (1993). *Lithostratigraphy of Indian Petroliferous Basins. Document II. West Rajasthan Basins* (pp. 1–123). Dehradun, India: KDMIPE, ONGC Publication.
- Misra, A. A., & Mukherjee, S. (2015). *Tectonic inheritance in continental rifts and passive margins. Springerbriefs in Earth Sciences*. Heidelberg: Springer International Publishing. ISBN 978-3-319-20576-2. <https://doi.org/10.1007/978-3-319-20576-2>
- Mohan, M. (1995). Cambay Basin – A promise of oil and gas potential. *Journal of the Palaeontological Society of India*, *40*, 41–47.
- Morgan, W. J. (1971). Convection plumes in the lower mantle. *Nature*, *23*, 42–43. <https://doi.org/10.1038/230042a0>
- Mukherjee, M. K. (1983). Petroleum prospects of Cretaceous sediments of the Cambay Basin, Gujarat, India. *Journal of Petroleum Geology*, *5*, 275–286. <https://doi.org/10.1111/j.1747-5457.1983.tb00572.x>
- Mukherjee, S., Misra, A. A., Calvès, G., & Nemčok, M. (2017). Tectonics of the Deccan Large Igneous Province: An introduction. In S. Mukherjee, A. A. Misra, G. Calvès, & M. Nemčok (Eds.), *Tectonics of the Deccan large igneous province. Geological Society, London, Special Publications*, *445*, 1–9.
- Najman, Y., Burley, S. D., Copley, A. C., Kelly, M. J., Pandey, K., & Mishra, P. (2018). The Oligocene unconformity of the Himalayan and NW Indian intraplate basins: A record of tectonics or mantle dynamics. *Tectonics*. <https://doi.org/10.1029/2018TC005286>
- O'Conner, J. E., Jones, M. A., & Haluska, T. L. (2003). Flood plain and channel dynamics of the Quinault and Queets Rivers, Washington, USA. *Geomorphology*, *51*, 31–59. [https://doi.org/10.1016/S0169-555X\(02\)00324-0](https://doi.org/10.1016/S0169-555X(02)00324-0)

- Pandey, D. K., Fursich, F. T., & Sha, J.-G. (2009). Interbasinal marker intervals – A case study from the Jurassic basins of Kachchh and Jaisalmer, western India. *Science in China Press*, 52, 1924–1931. <https://doi.org/10.1007/s11430-009-0158-0>
- Plummer, P. S., & Belle, E. R. (1995). Mesozoic tectono-stratigraphic evolution of the Seychelles microcontinent. *Sedimentary Geology*, 96, 73–91. [https://doi.org/10.1016/0037-0738\(94\)00127-G](https://doi.org/10.1016/0037-0738(94)00127-G)
- Plummer, P. S., Jospheph, P. R., & Samson, P. J. (1998). Depositional environments and oil potential of Jurassic/Cretaceous source rocks within the Seychelles microcontinent. *Marine and Petroleum Geology*, 15, 385–401. [https://doi.org/10.1016/S0264-8172\(98\)00019-1](https://doi.org/10.1016/S0264-8172(98)00019-1)
- Posmentier, H. E., & Kolla, V. (2003). Seismic geomorphology and stratigraphy of depositional elements in deep-water settings. *Journal of Sedimentary Research*, 73, 367–388. <https://doi.org/10.1306/111302730367>
- Racey, A., Fisher, J., Bailey, H., & Kumar-Roy, S. (2016). The value of fieldwork in making connections between onshore outcrops and offshore models: An example from India. *Geological Society of London, Special Publications*, 436, 21–53. <https://doi.org/10.1144/SP436.9>
- Rai, J. (2006). Discovery of nannofossils in a plant bed of the Bhuj Member, Kutch and its significance. *Current Science*, 91, 519–526.
- Rai, J., Singh, A., & Pandey, D. K. (2013). Early to middle Albian age calcareous nannofossils from Pariwar Formation of Jaisalmer Basin, Rajasthan, western India and their significance. *Current Science*, 105, 1604–1611.
- Rajanikath, A., & Chinnappa, C. H. (2016). Early Cretaceous flora of India – A review. *The Palaeobotanist*, 65, 209–245.
- Rajaram, M., Anand, S. P., Erram, V. C., & Shinde, B. N. (2016). Insight into the structures below the Deccan Trap-covered region of Maharashtra, India from geopotential data. *Geological Society of London*, 445, 219–236.
- Raju, A. T. R. (1968). Geological evolution of Assam and Cambay Tertiary Basins of India. *American Association of Petroleum Geology Bulletin*, 52, 2422–2437.
- Rao, K. M., Kumar, M. R., & Rastogi, B. K. (2015). Crust beneath the northwestern Deccan Volcanic Province India: Evidence for uplift and magmatic underplating. *Journal of Geophysical Research Solid Earth*, 120(5), 3385–3405. <https://doi.org/10.1002/2014JB011819>
- Reeves, C. (2014). The position of Madagascar within Gondwana and its movements during Gondwana dispersal. *Journal of African Earth Sciences*, 94, 45–57. <https://doi.org/10.1016/j.jafrearsci.2013.07.011>
- Reeves, C., & De-Wit, M. (2000). Making ends meet in Gondwana: Retracing the transforms of the Indian Ocean and reconnecting continental shear zones. *Terra Nova*, 12, 272–280. <https://doi.org/10.1046/j.1365-3121.2000.00309.x>
- Retallack, G. J. (1988). Field recognition of paleosols. *Geological Society of America Special Papers*, 216, 1–20.
- Retallack, G. J. (1990). *Soils of the past: An introduction to paleopedology*. Hammersmith, UK: Harper Collins Academic. <https://doi.org/10.1007/978-94-011-7902-7>
- Robinson, J. W., & McCabe, P. J. (2012). Evolution of a braided river system: The Salt Wash Member of the Morrison Formation (Jurassic) in southern Utah. *Society of Sedimentary Geology, Special Publication*, 59, 93–107.
- Roy, A. B., & Jokhar, S. R. (2002). *Geology of Rajasthan (Northwest India) Precambrian to recent*, Pawan Kumar. Jodhpur, India: Scientific Publishers, India.
- Schumm, S. A. (1981). Evolution and response of the fluvial system, sedimentologic implications. *The Society of Economic Paleontologists and Mineralogists, Special Publications*, 31, 19–29.
- Schumm, S. A. (1993). River response to baselevel change: Implications for sequence stratigraphy. *Journal of Geology*, 101, 279–294. <https://doi.org/10.1086/648221>
- Scotese, C. R. (2011). The PALEOMAP Project paleoatlas for ArcGIS, volume 2, Cretaceous paleogeographic and plate tectonic reconstructions. PALEOMAP Project, Arlington, TX.
- Scotese, C. R., Illich, H., Zumberge, J., & Brown, S. (2007). The GANDOLPH Project: One-year report: Paleogeographic and palaeoclimate controls on hydrocarbon source rock deposition, A report on the methods employed, the results of the paleoclimate simulations (FOAM) and oil/source rock compilation for the late Cretaceous (Cenomanian/Turonian; 93.5 Ma), late Jurassic (Kimmeridgian/Tithonian; 151 Ma), Early Permian (Sakmarin/Artinskian; 248 Ma) and late Devonian (Frasnian/Femennian; 372 Ma), Conclusions at the end of year one. Houston, TX: GeoMark Research Ltd.
- Sharma, K. K. (2007). K-T magmatism and basin tectonism in western Rajasthan, India: Results from extensional tectonics and not from Reunion plume activity. In G. R. Foulger & D. M. Jurdy (Eds.), *Plates, plumes and planetary processes. Geological Society of America Special Paper*, 430, 775–784.
- Sheth, H. C. (2007). Large Igneous Provinces (LIPs): Definition, recommended terminology and a hierarchical classification. *Earth Science Reviews*, 85, 117–124. <https://doi.org/10.1016/j.earscirev.2007.07.005>
- Simonetti, A., Bell, K., & Viladkar, S. G. (1995). Isotopic data from the Amba Dongar carbonatite complex, west-central India: Evidence for an enriched mantle source. *Chemical Geology*, 122, 185–198. [https://doi.org/10.1016/0009-2541\(95\)00004-6](https://doi.org/10.1016/0009-2541(95)00004-6)
- Singh, N. P. (2006). Mesozoic lithostratigraphy of the Jaisalmer Basin, Rajasthan. *Journal of the Palaeontological Society of India*, 51(2), 1–25.
- Sisodia, M. S., & Singh, U. K. (2000). Depositional environment and hydrocarbon prospects of the Barmer Basin, Rajasthan, India. *North American Free Trade Association*, 9, 309–326.
- Smewing, J.D., Warburton, J., Daley, T., Copestake, P., & Ul-haq, N. (2002). Sequence stratigraphy of the southern Kirthar Fold Belt and Middle Indus Basin, Pakistan: In P. D. Clift, D. Gaedicke & J. Craig (Eds.), *The tectonics and climatic evolution of the Arabian Sea Regions. Geological Society London, Special Publications*, 195, 273–299.
- Storey, M., Mahoney, J. J., Saunders, A. D., Duncan, R. A., Kelley, S. P., & Coffin, M. F. (1995). Timing of hot-spot related volcanism and the break-up and Madagascar and India. *Science*, 267, 852–855. <https://doi.org/10.1126/science.267.5199.852>
- Tabaei, M., & Singh, R. Y. (2002). Paleoenvironment and paleoecological significance of microforaminiferal linings in the Akli Lignite, Barmer Basin, Rajasthan, India. *Iranian International Journal of Science*, 3, 263–277.
- Tennvassås, I. (2018). *Characterisation of palaeosols in the Lower Cretaceous Helvetiafjellet Formation, Svalbard*. Master thesis, The University of Norway.

- Torsvik, T. H., Amundsen, H., Hartz, E. H., Corfu, C., Kuznir, N., Gaina, C., ... Jamtveit, B. (2013). A Precambrian microcontinent in the Indian Ocean. *Nature Geoscience*, 6, 223–227. <https://doi.org/10.1038/ngeo1736>
- Torsvik, T. H., Tucker, R. D., Ashwal, L. D., Carter, L. M., Jamtveit, B., Vidyadharan, T., & Venkataramana, P. (2000). Late Cretaceous India-Madagascar fit and timing of break-up and related magmatism. *Terra Nova*, 12, 220–225. <https://doi.org/10.1046/j.1365-3121.2000.00300.x>
- Tripathi, S. K. M., Kumar, M., & Srivastava, D. (2009). Palynology of Lower Palaeogene (Thanetian-Ypresian) coastal deposits from the Barmer Basin (Akli Formation, Western Rajasthan, India): Palaeoenvironmental and palaeoclimatic implications. *Geological Acta*, 7, 147–160.
- Wakefield, O. J. W., Hough, E., & Peatfield, A. W. (2015). Architectural analysis of a Triassic fluvial system: The Sherwood Sandstone of the East Midlands Shelf, UK. *Sedimentary Geology*, 327, 1–13. <https://doi.org/10.1016/j.sedgeo.2015.07.006>
- Wilson, A. A. (1993). The Merica mudstone group (trias) of the Cheshire Basin. *Proceedings of the Yorkshire Geological Society*, 49, 171–188. <https://doi.org/10.1144/pygs.49.3.171>
- Zaigham, N. A., Ahmad, M., & Hisam, N. (2012). Thar rift and its significance for hydrocarbons. American Association of Petroleum Geology Search and Discovery Article, 2014, Conference Paper.
- Zaigham, N. A., & Mallick, K. A. (2000). Prospect of hydrocarbon associated with fossil-rift structures of the southern Indus basin, Pakistan. *American Association of Petroleum Geology Bulletin*, 84, 1833–1848.

How to cite this article: Beaumont H, Clarke SM, Burley SD, Taylor AM, Mohapatra P. Sedimentology and the facies architecture of the Ghaggar-Hakra Formation, Barmer Basin, India: Implications for early Cretaceous deposition on the north-western Indian Plate margin. *Depositional Rec.* 2018; 00:1–31. <https://doi.org/10.1002/dep2.53>